A Thesis for the Degree of Doctor of Philosophy

Development of on-site detection system using a bi-functional linker-based gold nanoparticle aggregation system

이중기능링커 기반의 금 나노입자의 응집 시스템을 활용한 현장 검출법 개발

February, 2020

Jungwoo Hahn

Department of Agricultural Biotechnology

College of Agricultural and Life Sciences

Seoul National University

농학박사학위논문

Development of on-site detection system using a bi-functional linker-based gold nanoparticle aggregation system

이중기능링커 기반의 금 나노입자의 응집 시스템을 활용한 현장 검출법 개발

지도교수 최 영 진

이 논문을 박사학위논문으로 제출함

2020 년 2 월

서울대학교 대학원

농생명공학부

한정우

한정우의 박사학위논문을 인준함

2020 년 2 월

위 원 장	강 동 현	(인)
부위원장	최 영 진	(인)
위 원	유 상 열	(인)
위 원	김 용 노	(인)
위 원	김 영 록	(인)

Abstract

The average human life span is continuously increasing as are efforts worldwide to improve health and happiness, which has spurred the development of diagnostic technologies. In particular, great advances are being made in biosensors that enable on-site diagnosis. Biosensors, i.e., devices that examine analytes using biometric systems, typically consist of three components: detectors, transducers, and signal analysis systems. The goal for biosensors has evolved to enable biological sensing with high sensitivity and selectivity. The use of biosensor diagnostic technology developed for medical and point-of-care testing has been expanded and is now applied in various fields, including food safety, the military, and environmental monitoring. The development of biosensors in the field of food safety presents significant challenges because of the very diverse and complex matrices that characterize food. In other words, foods come in many varieties, and their composition matrices are complex and diverse, which makes it difficult for biosensors to operate. Therefore, biosensors in the field of food safety must be researched and developed based on our current understanding of food. Such a biosensor must require minimal pretreatment and be able to process a large number of samples without being affected by the food matrix. In addition, to be optimized for field application, the device must be miniature in size, automated, and simple to use.

Colorimetric methods that employ the strategy of gold nanoparticle (Au NP) aggregation have been determined to be suitable for field application because they can

perform signal analysis using only the naked eye and require no specialized analytical equipment. However, these methods are limited by their poor sensitivity for the following reasons: First, color can be distinguished by the naked eye only when using Au NPs at a concentration of about 10^{11} ea/mL or more. Second, in general, Au NPs facilitate both detection and signal analysis. As a result, high concentrations of Au NPs require high concentrations of analytes for signal analysis. Accordingly, a novel Au NP aggregation system is proposed that uses a bi-functional linker (BL), which has the same function as a switchable linker, and thus solves this problem by separating the signal analysis step from the analyte detection step by the aggregation of Au NPs. In addition, a BL-based assay, which has advantages such as simple operation and requiring no washing step, has emerged as a biosensor suitable for application in the food industry.

In this study, the aggregation strategy of using Au NPs as a BL showed that *Salmonella* Typhimurium could be detected in tomatoes at concentrations of less than 10 cells/400 μL within 45 minutes through simple manipulation. This indicates that this strategy is applicable to the food industry. In addition, prostate-specific antigen, a protein biomarker, was detected at a concentration of 100 fg/mL in a serum diluted to 1/10, which indicates that this strategy could be applied to various analytes. Finally, by detecting *Salmonella* Typhimurium using a miniaturized detection device with a 3-way valve chamber and a syringe filter, the BL-based assay could be applied in the field. Of course, to qualify this strategy for use in the food field, issues related to

automation, sample bulk-up, and stability must be addressed. However, the potential for field application is high due to this strategy's simplicity, sensitivity, and rapid diagnosis of analytes.

Key words: Gold nanoparticle (Au NP), aggregation, bi-functional linker (BL), on-site detection, naked eye

Student Number: 2012-23392

Contents

List of Tables

List of Figures

Chapter I. Introduction

I-1. Biosensors

I-1-1. Background of biosensors

As human life is prolonged, mankind is becoming more and more motivated to increase its levels of happiness and health. In this global social climate, the diagnostic technology market has made rapid progress during the last decade.[1, 2] In particular, to detect specific molecules, substances are detected at the molecular level using various types of bioreceptors such as enzymes, antibodies, antigens, receptors, and DNA.[3-8] The market for biosensors, devices that recognize interactions, is accelerating the pace of change due to the development and convergence of diagnostic and analytical technologies.[9, 10] Biosensor technology includes the diagnosis of infectious diseases, cancer, cardiovascular disease, and brain diseases; food safety identification; isotope immunoassays; coagulation; cytology; molecular diagnostics; blood grouping and typing; flow cytometry; and point-of-care testing.[11-22]

In addition, bio-diagnostic technology products include diagnostic kits for disease diagnosis, biochips, medical biosensors and ubiquitous disease management systems, and automated measurement systems.[23, 24] The development of biosensors was greatly advanced initially with the creation of medical diagnostic kits, but is now expanding into various fields such as food safety, environmental monitoring, and military use. In Table I-1, the characteristics of biosensors are identified with respect to their field of application.

Table I-1. Applications and characteristics of bio-sensors

Fields	Applications and characteristics	References
Medical treatment	-Takes advantage of the free movement of sensors and immediate cognitive characteristics for the areas in most demand, along with the use of medications and prompt medical treatment for critically ill patients -Analysis of biomaterials such as blood sugar, pregnancy hormones, cancer cells, cholesterol, and lactate	25
Environment	-Fast and efficient environmental substance detection over large areas -Minimizes air, water, and soil pollution and provides monitoring of comfortable living environments -Detects environmental substances such as environmental hormones (dioxin), waste water biological oxygen demand (BOD), heavy metals, and pesticides	26
Military	-Detects biological weapons that can be used for mass destruction such as sarin and anthrax.	27
Research	-Obtains information regarding biomolecules by measuring the interactions between biological materials such as DNA, RNA, antibodies, enzymes, and proteins.	28
Industrial Process	-Analysis of specific chemicals from each process, such as the biofermentation process, chemical plants, oil refineries, and pharmaceutical industries	29
Food	-Detects harmful substances such as residual pesticides, antibiotics, pathogens, heavy metals, and decaying substances in foods -The wide range of application calls for inexpensive, reliable, and easy-to-use sensors	30

I-1-2. Biosensors in the food field

To date, studies of biosensors have focused on increasing their sensitivity and selectivity.[31, 32] However, this research emphasis has slowed the application of biosensors in the food industry. Foods come in many varieties and are organized in complex matrixes.[33-35] Therefore, research on biosensors in the food industry requires a unique approach that incorporates the following elements: 1) development of biosensors that are minimally affected by the food matrix, 2) the study of food pretreatment, and 3) the study of the bulk-up of samples.[36-38] As yet, no biosensor can overcome these difficulties, and the demand for novel biosensors is very high since the food industry still detects foodborne pathogens using culture methods.

I-1-3. Biosensors for on-site detection

The rapid increase in pollutants, deadly diseases, and war chemicals around the world has generated a great demand for on-site sensing devices that can detect a variety of toxic chemicals and harmful bacteria in a very sensitive and specific manner.[39, 40] Significant advances in biosensor technology have facilitated a remarkable revolution in biomedical, environmental, and food safety in recent years.[36, 41, 42] In addition, biosensors have proven to be a valuable tool for detecting a variety of target analytes quickly and in real time with improved sensitivity and selectivity.[43, 44] Many challenges arise when using biosensors in the field. In the laboratory, biosensors operate in controlled conditions with respect to the environment and the

objects and devices used.[45] At application sites, however, the operation of biosensors can be inhibited by varied environments, uncontrolled matrices, and the state of the sample.[46] To address these challenges, the development of small, portable, user-friendly, and automated sensing devices for the on-site detection of targets is increasing.

I-2. Colorimetric assay in the food safety field

I-2-1. Methods for the identification of food-borne pathogens

It is estimated that foodborne infections cause more than 76 million illnesses, more than 300,000 hospitalizations, and 5,000 deaths each year in the United States alone.[47, 48] However, only some of these food poisoning infections are diagnosed and officially reported.[49] Conventional tests for the identification of food-borne pathogens are culture-based methods that require the individual biochemical identification of species in a large number of isolated colonies. These methods are labor-intensive and time-consuming and require specific and unique primary detection methods. To solve these problems, various methods have been proposed, such as immunoblotting, the enzyme-linked immunosorbent assay (ELISA), and electrochemical analysis.[50-53] These methods overcome the problem of identification, but are not always good choices because of their lack of sensitivity or specificity.

I-2-2. Au NP-based colorimetric biosensing strategy

A colorimetric assay can be a very simple and fast approach in that results are detected by the naked eye without any complicated equipment. Gold nanoparticles (Au NPs) have been selected as a sensing material for the colorimetric detection of various analytes such as DNA, protein, and pathogens because of their unique optical properties, ease of surface modification, and high surface/volume ratio. The small Au

NPs of colloids (usually 10–50 nm in diameter) appear dark red in color, and have attracted interest since ancient times. Localized surface plasmon resonance (LSPR), the essence of the optical property of Au NPs, is caused by the collective oscillation of the nanostructure's conduction-band electron gases in resonance with the incident electromagnetic field.[54] Small Au NPs (e.g., 13 nm in diameter) absorb green light, which corresponds to a strong absorption band (surface plasmon band) at ~520 nm in the visible light spectrum. Thus, the Au NP solution appears red in color. Since small Au NPs are governed by their unique LSPR, attractive colorimetric reactions are possible via changes in the shape, size, composition, and interparticle distance of Au NPs, as well as the dielectric constant (refractive index) of the surrounding medium.[55-57] The contribution of different parameters to the total extinction of Au NPs is described by the Mie theory.[58-62] Through the LSPR phenomenon, Au NPs appear red or blue. This phenomenon correlates with the coherent oscillation of the surface electrons (localized surface plasmons) of Au NPs induced by the incident electromagnetic field. The surface electrons of certain small Au NPs resonate with the incoming specific light in the dipole mode. That is, Au NPs of a certain size absorb a specific wavelength (surface plasmon band) of green light in the visible light spectrum and emit a red color by the resonance of the surface electrons of Au NPs. As the size of the Au NPs increases, they enter the visible light spectrum, which resonates with the surface electrons of the Au NPs and causes a red shift and broadening of the surface plasmon band.[63, 64] This also can explain the red shift and color change (red to

purple) induced by the aggregation of Au NPs.[65] The aggregation reaction of Au NPs can greatly facilitate the induction of a color change, which is one of the most widely used strategies in Au NP-based colorimetric biosensing assays. There are two main strategies for inducing the aggregation of Au NPs: the inter-particle crosslinking aggregation mechanism and the non-crosslinking aggregation mechanism.[66] The inter-particle crosslinking aggregation mechanism is a method for inducing aggregation by the crosslinking of Au NPs using a specific mediator, such as DNA, protein, or antibodies. This method is widely used in biosensing assays because it enables control of the degree of aggregation. The non-crosslinking aggregation mechanism is a method for inducing the aggregation of Au NPs by inducing their destabilization by changing the surface charge or electro-steric hindrance.

This method offers several advantages. First, aggregation can be induced rapidly, and the reaction can be completed in a few minutes. Second, there is no need to implement bio-receptors capable of binding particles at multiple binding sites. The development of Au NP-based colorimetric biosensing involves the selection of these two mechanisms as the main strategy, depending on the desired purpose.

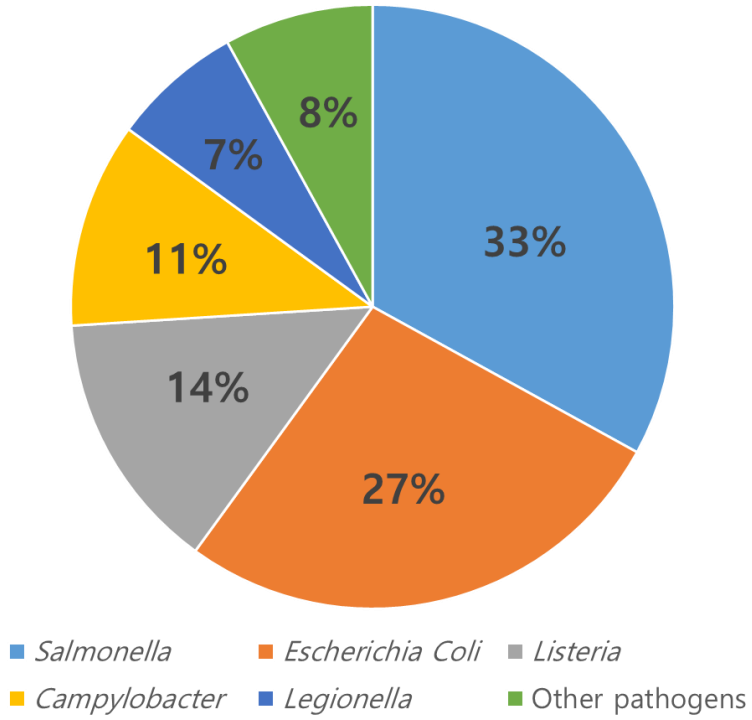

Source: ISI Web of Science. *ca*. 2500 Articles found on pathogen detection over the last 20 years

Figure I-1. Primary detection methods that indicate the presence of *Salmonella* and *E. Coli*.

I-2-3. Au NP-based colorimetric bio-sensing in food safety

The detection of target analytes in the field of food safety has been explored using the Au NP aggregation-based colorimetric assay. Indeed, the broad spectrum of chemical hazards has been explored as well as the detection of pathogens, DNA, toxins, and proteins of high importance in the food safety field. In developed countries, outbreaks caused by food-borne pathogens and their toxins are most commonly reported, which predominantly involve enteric viruses, a non-typhoidal *Salmonella* enterica, and *Campylobacter* spp., followed by staphylococcal enterotoxins, *Clostridium* perfringens, pathogenic *Escherichia coli* (particularly enterohemorrhagic pathotypes), *Bacillus cereus*, *Vibrio* parahaemolyticus, and marine toxins.[67, 68] In general, *Escherichia coli* is the most thoroughly studied model bacterium, but as shown in Figure I-1, *Salmonellae* is also a model bacterium for which many detection studies have been reported. There is a need for more effective methods for screening chemical and biological contaminants in the real world, where specialized equipment is not always available, and the colorimetric assay based on Au NP aggregation can be a very good alternative. Table I-2 shows a representative Au NP-based colorimetric assay for the detection of pathogens. Many of these reports have focused on the functionalization of Au NPs in line with their aggregation strategy. Kim and colleagues stabilized Au NPs by applying aptamers that have a binding ability to *Campylobacter*. Using this method, the non-crosslinking aggregation of Au NPs was

induced according to the presence or absence of a target. Su and colleagues used a crosslinking aggregation strategy to detect *E. coli* O157:H7 by attaching it to mercaptoethylamine, which can bind Au NPs. Table I-2 lists the biosensing applications performed using the Au NP aggregation strategy, which shows the advantages of a very simple detection results that can be visually confirmed as a suitable technique for field application. However, in existing Au NP-based colorimetric assays, it is not only difficult to confirm a quantitative relationship, as it is based on a visual check of the color change, but its sensitivity is also poor. Thus, there is a need for the development of novel Au NP-based colorimetric assays.

Table I-2. Food-borne pathogen sensing based on Au NP aggregation

Analyte	Sample	Detection analytical principle		Analytical performance	Ref.
		Functionalization	Interaction		
Campylobacter	Chicken carcass	Label-free	Electrostatic adsorption (aptamer)	Reduces the detection time to 30 min after enrichment	63
Escherichia coli O157:H7	Acetate buffer	Mercaptoethylamine-modified Au NPs	Mercaptoethylamine—target	Less than 5 min from bacterium binding to detection	64
Escherichia coli O157:H7	Yellow corn	Antibody-modified Au NPs	Antibody—antigen	Optical signals monitored by the naked eye, resulting in a dramatic color change from red to blue	65
Listeria monocytogenes	Milk	Hyperbranching rolling circle amplification (HRCA) combined Au NPs	Electrostatic adsorption (HRCA—*hly* gene target)	Simplicity and high sensitivity	66
Salmonella Typhimurium	Milk	Aptamer combined Au NPs	Electrostatic adsorption (NaCl)	LOD = 56 cfu/mL	67

I-3. Bi-functional linker-based assay

To address the limitations of colorimetric methods using the Au NP aggregation strategy, our research group designed a switchable linker (SL) that functions in the same way as a bi-functional linker (BL) in that it can induce the color-shading effect. The BL, which is the core of this system, must satisfy three conditions. First, it must crosslink the nanoparticles; secondly, it must be able to bind to the analyte; and lastly, when combined with the analyte, the system's ability to crosslink the nanoparticles must be constrained. I refer to this situation as the linker being switched off. When this condition occurs, two phenomena result: First, the quantitative relationship between the linker and the Au NPs changes, and second, as the relationship changes, the range of the linker concentration exhibiting visual color change (REVC) shifts in the direction of high linker concentrations. Therefore, BL-based assays can detect targets visually and semi-quantitatively. As such, in this study, to overcome the limitations of the existing colorimetric method, I evaluated the potential for field application of the BL-based assay.

I-4. References

1. B. D. Malhotra and A. Chaubey, *Sensors and Actuators B: Chemical*, 2003, 91, 117-127.
2. P. Yager, G. J. Domingo and J. Gerdes, *Annual review of biomedical engineering*, 2008, 10.
3. M. Hasanzadeh, N. Shadjou, M. Eskandani and M. de la Guardia, *TrAC Trends in Analytical Chemistry*, 2012, 40, 106-118.
4. J. H. Kim, S. Y. Lim, D. H. Nam, J. Ryu, S. H. Ku and C. B. Park, *Biosensors and Bioelectronics*, 2011, 26, 1860-1865.
5. P. B. Luppa, L. J. Sokoll and D. W. Chan, *Clinica chimica acta*, 2001, 314, 1-26.
6. N. Parmin, U. Hashim, S. C. Gopinath and M. Uda, in *Nanobiosensors for Biomolecular Targeting*, Elsevier, 2019, pp. 195-210.
7. T. Vo-Dinh, *Sensors and Actuators B: Chemical*, 1998, 51, 52-59.
8. T. Vo-Dinh and B. Cullum, *Fresenius' journal of analytical chemistry*, 2000, 366, 540-551.
9. P. Bhatia and A. Chugh, *Curr. Synthetic Syst. Biol*, 2013, 1, 2332-0737.1000108.
10. S. Kumar, S. Kumar, M. A. Ali, P. Anand, V. V. Agrawal, R. John, S. Maji and B. D. Malhotra, *Biotechnology journal*, 2013, 8, 1267-1279.
11. E. B. Bahadır and M. K. Sezgintürk, *Analytical biochemistry*, 2015, 478, 107-120.
12. B. Bohunicky and S. A. Mousa, *Nanotechnology, science and applications*, 2011, 4, 1.
13. S. Choi, M. Goryll, L. Y. M. Sin, P. K. Wong and J. Chae, *Microfluidics and Nanofluidics*, 2011, 10, 231-247.
14. J. Durner, *Angewandte Chemie International Edition*, 2010, 49, 1026-1051.
15. D. J. Ecker, R. Sampath, H. Li, C. Massire, H. E. Matthews, D. Toleno, T. A. Hall, L. B. Blyn, M. W. Eshoo and R. Ranken, *Expert review of molecular diagnostics*, 2010, 10, 399-415.
16. T. Fodey, P. Leonard, J. O'Mahony, R. O'Kennedy and M. Danaher, *TrAC Trends in Analytical Chemistry*, 2011, 30, 254-269.
17. M. Fraga, N. Vilariño, M. C. Louzao, L. P. Rodríguez, A. Alfonso, K. Campbell, C. T. Elliott, P. Taylor, V. Ramos and V. Vasconcelos, *Analytica chimica acta*, 2014, 850, 57-64.
18. M. Li, J. Tian, M. Al-Tamimi and W. Shen, *Angewandte Chemie international edition*, 2012, 51, 5497-5501.
19. Y. Luo, L. Zhang, W. Liu, Y. Yu and Y. Tian, *Angewandte Chemie International Edition*, 2015, 54, 14053-14056.
20. A. Qureshi, Y. Gurbuz and J. H. Niazi, *Sensors and Actuators B: Chemical*, 2012, 171, 62-76.

21. L. Yang, X. Huang, L. Sun and L. Xu, *Sensors and Actuators B: Chemical*, 2016, 224, 863-867.
22. C. Yao, L. Qu and W. Fu, *Sensors*, 2013, 13, 6946-6956.
23. F. S. R. R. Teles, *Analytica chimica acta*, 2011, 687, 28-42.
24. M. Zarei, *TrAC Trends in Analytical Chemistry*, 2017, 91, 26-41.
25. J. Kim, S. Imani, W. R. de Araujo, J. Warchall, G. Valdés-Ramírez, T. R. Paixão, P. P. Mercier and J. Wang, *Biosensors and Bioelectronics*, 2015, 74, 1061-1068.
26. J.-Z. Sun, G. Peter Kingori, R.-W. Si, D.-D. Zhai, Z.-H. Liao, D.-Z. Sun, T. Zheng and Y.-C. Yong, *Water Science and Technology*, 2015, 71, 801-809.
27. P. Mehrotra, *Journal of oral biology and craniofacial research*, 2016, 6, 153-159.
28. K. Reder-Christ and G. Bendas, *Sensors*, 2011, 11, 9450-9466.
29. P. R. Coulet and L. J. Blum, *Biosensor principles and applications*, CRC Press, 2019.
30. B. Van Dorst, J. Mehta, K. Bekaert, E. Rouah-Martin, W. De Coen, P. Dubruel, R. Blust and J. Robbens, *Biosensors and Bioelectronics*, 2010, 26, 1178-1194.
31. J. Chen, J. Zhang, J. Li, F. Fu, H.-H. Yang and G. Chen, *Chemical Communications*, 2010, 46, 5939-5941.
32. Y. Zhou, L. Tang, G. Zeng, J. Chen, Y. Cai, Y. Zhang, G. Yang, Y. Liu, C. Zhang and W. Tang, *Biosensors and Bioelectronics*, 2014, 61, 519-525.
33. L. W. Aurand, *Food composition and analysis*, Springer Science & Business Media, 2013.
34. M. J. Rein, M. Renouf, C. Cruz-Hernandez, L. Actis-Goretta, S. K. Thakkar and M. da Silva Pinto, *British journal of clinical pharmacology*, 2013, 75, 588-602.
35. A. Wilkowska and M. Biziuk, *Food chemistry*, 2011, 125, 803-812.
36. R. Pilolli, L. Monaci and A. Visconti, *TrAC Trends in Analytical Chemistry*, 2013, 47, 12-26.
37. K. Warriner, S. M. Reddy, A. Namvar and S. Neethirajan, *Trends in food science & technology*, 2014, 40, 183-199.
38. B. J. Yakes, J. Deeds, K. White and S. L. DeGrasse, *Journal of agricultural and food chemistry*, 2010, 59, 839-846.
39. K. Kim, O. G. Tsay, D. A. Atwood and D. G. Churchill, *Chemical reviews*, 2011, 111, 5345-5403.
40. R. K. Mishra, L. J. Hubble, A. Martín, R. Kumar, A. Barfidokht, J. Kim, M. M. Musameh, I. L. Kyratzis and J. Wang, *ACS sensors*, 2017, 2, 553-561.
41. J. Kirsch, C. Siltanen, Q. Zhou, A. Revzin and A. Simonian, *Chemical Society Reviews*, 2013, 42, 8733-8768.
42. S. Vigneshvar, C. Sudhakumari, B. Senthilkumaran and H. Prakash, *Frontiers in bioengineering and biotechnology*, 2016, 4, 11.
43. V. Perumal and U. Hashim, *Journal of applied biomedicine*, 2014, 12, 1-15.

44. X. Zhao, C.-W. Lin, J. Wang and D. H. Oh, *J. Microbiol. Biotechnol*, 2014, 24, 297-312.
45. J. Arlett, E. Myers and M. Roukes, *Nature nanotechnology*, 2011, 6, 203.
46. V. Scognamiglio, G. Pezzotti, I. Pezzotti, J. Cano, K. Buonasera, D. Giannini and M. T. Giardi, *Microchimica Acta*, 2010, 170, 215-225.
47. P. S. Mead, L. Slutsker, V. Dietz, L. F. McCaig, J. S. Bresee, C. Shapiro, P. M. Griffin and R. V. Tauxe, *Emerging infectious diseases*, 1999, 5, 607.
48. S. P. Oliver, K. J. Boor, S. C. Murphy and S. E. Murinda, *Foodborne pathogens and disease*, 2009, 6, 793-806.
49. X.-W. Wang, L. Zhang, L.-Q. Jin, M. Jin, Z.-Q. Shen, S. An, F.-H. Chao and J.-W. Li, *Applied microbiology and biotechnology*, 2007, 76, 225.
50. I. Diaconu, C. Cristea, V. Hârceagă, G. Marrazza, I. Berindan-Neagoe and R. Săndulescu, *Clinica Chimica Acta*, 2013, 425, 128-138.
51. Y. Li, M. Hong, Y. Lin, Q. Bin, Z. Lin, Z. Cai and G. Chen, *Chemical Communications*, 2012, 48, 6562-6564.
52. S. Mattiucci, M. Paoletti, A. Colantoni, A. Carbone, R. Gaeta, A. Proietti, S. Frattaroli, P. Fazii, F. Bruschi and G. Nascetti, *BMC infectious diseases*, 2017, 17, 530.
53. S. Sadir, M. P. Prabhakaran, D. H. Wicaksono and S. Ramakrishna, *Sensors and Actuators B: Chemical*, 2014, 205, 50-60.
54. C. Bohren, D. Huffman and Z. Kam, *Nature*, 1983, 306, 625.
55. J. Anker, W. Hall and O. Lyandres, *Nat Mater*, 2008, 7, 442.
56. M. E. Stewart, C. R. Anderton, L. B. Thompson, J. Maria, S. K. Gray, J. A. Rogers and R. G. Nuzzo, *Chemical reviews*, 2008, 108, 494-521.
57. K. A. Willets and R. P. Van Duyne, *Annu. Rev. Phys. Chem.*, 2007, 58, 267-297.
58. S. K. Ghosh and T. Pal, *Chemical reviews*, 2007, 107, 4797-4862.
59. N. J. Halas, S. Lal, W.-S. Chang, S. Link and P. Nordlander, *Chemical reviews*, 2011, 111, 3913-3961.
60. P. K. Jain, K. S. Lee, I. H. El-Sayed and M. A. El-Sayed, *The journal of physical chemistry B*, 2006, 110, 7238-7248.
61. J. J. Storhoff, A. A. Lazarides, R. C. Mucic, C. A. Mirkin, R. L. Letsinger and G. C. Schatz, *Journal of the American Chemical Society*, 2000, 122, 4640-4650.
62. Y. Sun and Y. Xia, *Analyst*, 2003, 128, 686-691.
63. C.-C. Huang, Y.-F. Huang, Z. Cao, W. Tan and H.-T. Chang, *Analytical chemistry*, 2005, 77, 5735-5741.
64. V. Pavlov, Y. Xiao, B. Shlyahovsky and I. Willner, *Journal of the American Chemical Society*, 2004, 126, 11768-11769.
65. A. Gole and C. J. Murphy, *Langmuir*, 2005, 21, 10756-10762.
66. W. Zhao, M. A. Brook and Y. Li, *ChemBioChem*, 2008, 9, 2363-2371.
67. C. EFSA, *EFSA*, 2010, 8, 1-370.

68. C. OutbreakNet.
69. Y.-J. Kim, H.-S. Kim, J.-W. Chon, D.-H. Kim, J.-Y. Hyeon and K.-H. Seo, *Analytica chimica acta*, 2018, 1029, 78-85.
70. H. Su, Q. Ma, K. Shang, T. Liu, H. Yin and S. Ai, *Sensors and Actuators B: Chemical*, 2012, 161, 298-303.
71. M. Ali, T. A. S. Eldin, G. E. Moghazy, I. M. Tork and I. Omara, *Int. J. Curr. Microbiol. App. Sci*, 2014, 3, 697-708.
72. Z. Fu, X. Zhou and D. Xing, *Methods*, 2013, 64, 260-266.
73. X. Ma, L. Song, N. Zhou, Y. Xia and Z. Wang, *International journal of food microbiology*, 2017, 245, 1-5.

Chapter II. A bi-functional linker based immunoassay for ultrasensitive visible detection of *Salmonella* in tomatoes

Published in Journal of Food Science

(J. Hahn, E. Kim, Y.S. You, S. Gunasekaran, S. Lim, and Y. J. Choi, *J. Food Science.* 2017, 82, 10, 2321-2328)

II-1. Introduction

Recently, interest in healthier lifestyles has led to an increase in the consumption of fresh produce, including tomatoes, due to the associated health benefits. a Ironically, this increase has also been associated with increased potential for outbreaks of fresh produce-related foodborne illness. [1-4] Among foodborne pathogens, *Salmonella* is one of the greatest concerns associated with fresh produce due to its high potential for growth before consumption and the low infectious dose necessary to cause illness. [5] *Salmonella* infection from tomatoes has increased markedly in both incidence and severity in recent decades. Between 2004 and 2010, 21 *Salmonella* outbreaks related to tomatoes occurred in the United States. Such produce is commonly intended to be consumed fresh, without a kill step. [6, 7] Therefore, the systematic on-site detection of *Salmonella* in fresh tomatoes after harvesting or before processing is important.

There are several difficulties associated with detecting *Salmonella* in the food system, especially on tomatoes. First, the contents of a tomato include carbohydrates, proteins, and inorganic substances, which can inhibit sensing systems using antibodies and DNA probes. [8-10] Second, a sensing system that evaluates proteins or DNA could be affected by unfavorable environmental conditions such as the acidic pH of a tomato. [11] Third, the red color of the tomato could interfere with the visible signal in a colorimetric sensing system, such as a gold nanoparticle (Au NP) aggregation strategy

using a color change from red to purple. [12] To overcome these difficulties, considerable effort has been directed to practical, rapid, and sensitive means of detecting pathogens.

These problems with real food have prompted researchers to seek novel techniques for detecting *Salmonella*, including enzyme-linked immunosorbent assays [13-15], polymerase chain reaction [16, 17], and oligonucleotide probes [17-19] for DNA of the target pathogen. Although these methods are rapid and specific, they have limitations for use in real food systems, including a high limit of detection. [20 21, 22] A low LOD is important for the contamination pathway of *Salmonella* on tomatoes.

During production, processing, and distribution, tomatoes can be contaminated with *Salmonella* serotypes such as Javiana, Montevideo, Newport, and Typhimurium through many possible sources, including contaminated water, infected food handlers, and contact with surfaces contaminated with the feces of domestic animals, ruminants, or rodents. [23-26] The cross-contamination concentration of *Salmonella* on tomatoes is less than 10^3 CFU/g. However, there is a sharp increase to 10^6–10^7 CFU/g at room temperature, on transportation, after maturity, or during display in retail shops. [6, 27] Therefore, a fast, accurate, and convenient method of detecting a low density of *Salmonella* on tomatoes is necessary to ensure product safety.

Previously, our research group introduced the concept of implementing a switchable linker (SL) as same as a bi-functional linker (BL) to improve visible

detection methods by controlling the extent of nanoparticle aggregation. [28] The BL can induce large-scale nanoparticle aggregation based on the quantitative relationship among the BLs, nanoparticles, and target. When BLs are switched off by the target, the relationship changes, which shifts the range of linker concentration exhibiting visual color change (REVC). Based on this concept, I developed a novel BL-based immunoassay that improves the ultrasensitive detection of *Salmonella* to overcome the difficulties with whole tomato samples. Here, I evaluated whether the BL-based immunoassay was rapid and simple, and had a low detection limit for in-field, rather than laboratory, analysis.

II-2. Materials and Methods

II-2-1. Chemicals, reagents, and instruments

Bovine serum albumin (BSA), 1 mM tetrachloroaurate, phosphate-buffered saline (PBS), polyethylene glycol 2000, Tween 20, and streptavidin were purchased from Sigma-Aldrich (Madison, WI). Tetraborate pH standard solution was purchased from Wako Pure Chemicals (Osaka, Japan). Anti-*Salmonella* antibody (biotin) was purchased from Abcam (Cambridge, MA). Trisodium citrate, vials, and ethanol were purchased from local suppliers.

The buffer used for Au NP synthesis was sterilized distilled water prepared with 1% (w/v) trisodium citrate for reducing. The buffers used for the BL-based immunoassay were 0.01 mol/L PBS (pH 7.4) prepared with 0.5% (w/v) BSA for blocking, and 0.01 mol/L tetraborate pH standard solution (pH 7.4) for diluting streptavidin. The buffer used for reducing cell aggregates was prepared PBS buffer containing 2% PEG 2000 and 0.02% Tween 20.

The BL-based immunoassay was performed in vials (4science, South Korea). The assay absorbance was read by a UV-1700 spectrophotometer (Shimadzu, Japan). A vortex mixer (Hanil Lab Tech, South Korea) was used for inducing the aggregation of Au NPs. A stomacher (Interscience, France) was used for the homogenization of samples.

II-2-2. Preparation of streptavidin-coated Au NPs

Spherical Au NPs were prepared by reducing 1 mM tetrachloroaurate with 1% (w/v) trisodium citrate. [29] The synthesized Au NPs had an ultraviolet–visible (UV-Vis) spectrum peak at approximately 520 nm, which corresponds to an average diameter of 13 nm. The Au NPs (~13 nm in diameter) were coated with 0.2 μg/mL streptavidin dissolved in tetraborate solution at pH 7.4 and washed repeatedly to remove unbound streptavidin. The Au NPs functionalized with multiple streptavidin molecules (st-Au NPs) had an absorption peak at approximately 531.5 nm. They were stored in 0.5% (w/v) BSA dissolved in PBS at concentrations giving a peak absorbance value of 0.43 on the UV-Vis spectra for samples at 1:10 dilution. The concentration of Au NPs used in the experiment was about 7×10^{12} particles/mL.

II-2-3. Bacterial strain and culture conditions

The bacterial strain used in the assay was *Salmonella* Typhimurium (ATCC 19585). Other *Salmonella* strains used to test the selectivity of the assay included *Salmonella* Newport (ATCC 27869) and *S.* Javiana (ATCC 10721). *Staphylococcus aureus* (ATCC 12600), *Escherichia coli* K-12 MG1655 (ATCC 47076), and *E. coli* DH5α (ATCC 47093) were also used in the selectivity test. All bacterial strains were purchased from ATCC. These strains were grown in tryptic soy broth medium (pH 7.3, TSB, Difco Laboratories) at 37 ± 1℃ for 24 h. The number of viable cells in the culture was determined by a microbial plate count, and the final suspensions contained

a bacterial concentration of 3×10^9 CFU/mL. These cultures were used to inoculate the tomato samples.

II-2-4. Artificial inoculation of tomato samples with *Salmonella*

Tomatoes (Solanum lycopersicum), each about 200 g, were purchased at a local grocery store and stored for a maximum of 3 days at 25 ± 1℃ before being used in tests. Prepared tomatoes were washed five times with 70% ethanol and DW to eliminate all possible contaminants. [30] Next, the tomatoes with the end of the stem were placed on clean paper (15 × 15 cm) inside a biosafety hood and dried for 30 min. One milliliter of the final inoculum was inoculated in 15 approximately identical volumes on the tomato surface using a micropipette. [31] Tomatoes were dried in the hood at 25℃ for 30 minutes to prevent bacterial losses.

Two control groups were used in this experiment. First, the level of background microflora present on the tomatoes was determined as an uninoculated control. Second, a control group was set up to compare the inoculated and untreated samples. The inoculated tomato samples and two controls were mixed with 100 mL of 0.1% sterilized peptone in a sterilized stomaching bag (Fisher Scientific, Pittsburgh, PA) and homogenized by hand with sterilized gloves for 2 minutes until completely crushed and homogenized. An experiment comparing homogenization methods is described below and the results are shown in Table S1. The final cell densities on the

tomato samples ranged from 10^3 to 10^5 CFU/EA. The BL-based immunoassay described above was performed using 5 mL of each sample in a sterile test tube.

The remaining bacterial populations in the tomato were evaluated in both a nonselective medium (tryptic soy agar, Difco Laboratories) and a selective medium (xylose lysine deoxycholate, Difco Laboratories) for S. Typhimurium. Media were incubated at 37℃ for 24 h and then colonies were counted.

The different species used in the selectivity experiment were evaluated on each appropriate selective medium: cefixime-tellurite sorbitol MacConkey agar (CT-SMAC, Difco Laboratories) for E. coli K-12 MG1655 and E. coli DH5α, xylose lysine deoxycholate (XLD, Difco Laboratories) for S. Javiana and S. Newport, and Baird-Parker agar (BPA, Difco Laboratories) for S. aureus.

II-2-5. Comparison of homogenization methods

To validate the effectiveness of the hand-mashing homogenization method, I compared three different homogenization methods: mashing tomatoes by hand, stomaching without peptone water, and stomaching with peptone water (1:10 dilution). Each whole tomato weighing approximatively 200 g was added to a sterile stomach bag and hand-mashed and homogenized vigorously for 2 min. Two other conventional homogenization methods using a stomacher (230 rpm, 2 min) to homogenize tomato produce were used: one did not use peptone water and the other used 2% peptone

water. One milliliter of the tomato sample was taken randomly from the three methods and plate counts were performed.

II-2-6. Time for large-scale aggregation using st-Au NPs and b-Ab

I measured the time required for the large-scale aggregation of the nanoparticles with and without agitation. Under the former condition, samples were gently agitated in a vortex mixer at 200 rpm. Non-agitated samples were measured every 15 min for 2 h, and agitated samples were measured every minute for 5 min. The results of the two experiments were recorded as images, and the absorbance at 531. 5 nm (*i.e*., the absorbance peak of the st-Au NPs) was measured only for those samples prepared without agitation. The concentration of BLs used in the experiment was the same as that in the BL-based immunoassay described below.

II-2-7. Selectivity of b-Ab as a bi-functional linker

To determine the selectivity of the BL-based immunoassay, the rabbit polyclonal anti-*Salmonella* biotinylated antibody (b-Ab) used as the BL was exposed to six strains of bacteria at concentrations of 10^5 CFU/mL: *Salmonella* Typhimurium (ATCC 19585), *S.* Newport (ATCC 27869), *S.* Javiana (ATCC 10721), *Staphylococcus aureus* (ATCC 12600), *E. coli* K-12 MG1655 (ATCC 47076), and *E. coli* DH5α (ATCC 47093). B-Ab (15 and 25 μg/mL) was added to the following seven solutions: negative control (PBS) and single-culture solutions of *Salmonella*

Typhimurium, *S*. Newport, *S*. Javiana, *Staphylococcus aureus*, *E*. *coli* K-12 MG1655, and *E*. *coli* DH5α. After 30 min, st- Au NPs were added to each sample. The peak absorbance of the mixture was measured with a UV-Vis spectrophotometer 120 min after adding the st- Au NPs, and the difference in absorbance between the two concentrations was calculated.

II-2-8. BL-based immunoassay

Salmonella polyclonal antibody with biotin as the BL was used in this assay. Figure II-1 shows a schematic of the BL-based immunoassay. Briefly, the assay was performed in a total reaction volume of 400 µL containing 200 µL of st-Au NP solution at a fixed concentration, 100 µL of b-Ab, and 100 µL of a test sample (either PBS at pH 7.4 or a tomato sample at pH 4.3). First, 100 µL of the test sample was mixed with 100 µL of b-Ab at various concentrations. After an adequate reaction time (>30 min) without agitation, I added 200 µL of st-Au NPs to the mixture, and then let the sample stand for 2 h. The color change of the reaction was monitored to determine the quantitative correlation among samples, BLs, and st Au NPs.

In BL-based assays, it is important to determine the REVC of the BL. Hence, before applying an BL-based immunoassay for the detection of *Salmonella* in fresh tomato samples, the REVC was determined for the BL used in this study (Figure II-S1). To determine the REVC, an assay was performed in PBS at various b-Ab concentrations (14–52 µg/mL). BL concentrations of 16, 18, 20, 36, 38, and 40 µg/mL

in PBS were selected as the concentrations most likely to show the differences in REVC, and BL concentrations of 16 and 18 μg/mL were used for the tomato samples. Based on the REVC, these concentrations were determined to be the most effective for the simple on-site detection of *Salmonella* in tomato samples.

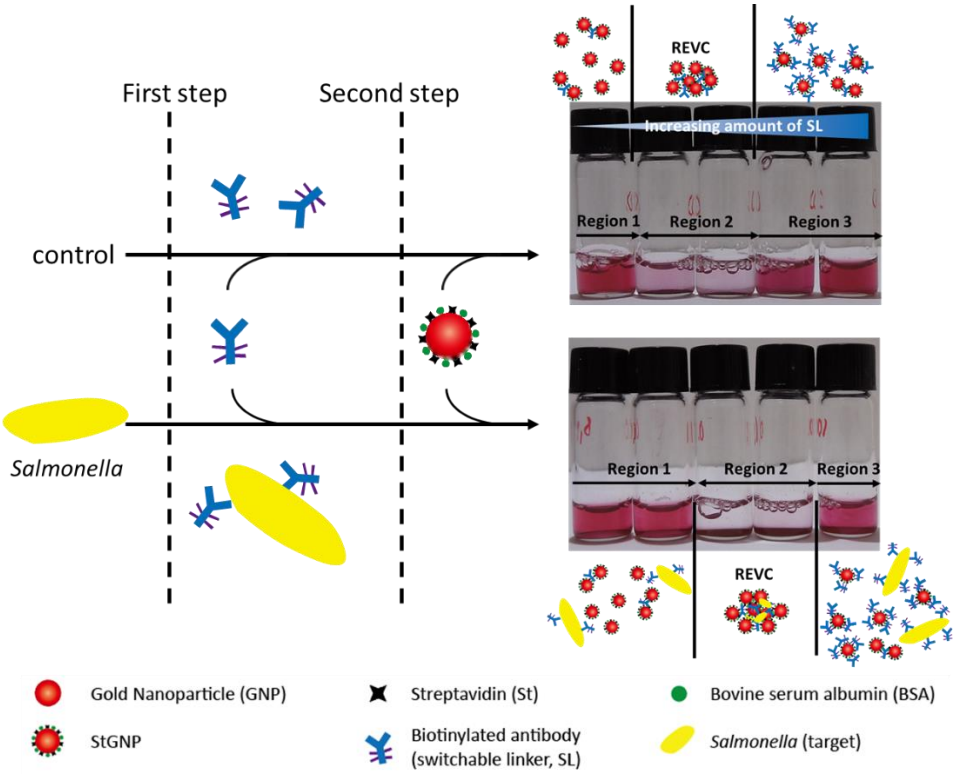

Figure II-1. Schematic representation of a switchable linker (SL) or bi-functional linker (BL)-based immunoassay. First, the biotinylated *Salmonella* antibody (the BL) was added to solutions that either contained the target or did not. Then, functionalized nanoparticles (st-Au NP) were added to the solutions.

II-2-9. Validation test

To validate the detection of a low density of *Salmonella*, single-cell detection was applied with slight modification. [32] Briefly, *Salmonella* was inoculated in LB broth and incubated at 37℃ for expansion. Bacterial cells were collected when the OD_{600} reached 0.5–0.8. The collected cells were repeatedly resuspended by pipetting and washed repeatedly with PBS buffer containing 2% PEG 2000 and 0.02% Tween 20 to reduce cell aggregates. The bacterial cells were resuspended to 1 OD_{600} with PBS buffer. The cell density of 1 OD_{600} was determined by a plate count. The cell suspension was then serially diluted to 10 cells/100 μL. The 100-μL volumes of diluted bacterial suspensions containing approximately 10 bacterial cells were confirmed by plate counts and the BL-based immunoassay simultaneously. In the BL-based immunoassay, 100 μL of diluted suspension was further diluted to 3,000 μL and divided equally into 30 vials. Each vial was then analyzed using the assay to determine whether it contained bacteria at the peak measured with a UV-Vis spectrophotometer. The positive vials were recorded and considered to contain a single cell each.

II-2-10. Statistical analysis

The various treatments and groups were compared using one-way analysis of variance followed by Duncan's test. Differences of $p < 0.05$ were considered statistically significant. The statistical analysis was performed using SPSS Statistics

ver. 23.0 (IBM, Armonk, NY, USA). The data represent an average of at least three independent experiments or measurements. The results are expressed as the mean ± standard deviation (SD).

II-3. Results and Discussion

II-3-1. The principle of BL-based immunoassay

BL-based immunoassay uses BLs to induce large-scale aggregation of Au NPs. BLs are cross-linkers that not only induce large-scale aggregation of Au NP but also recognize a target. BLs can induce large-scale aggregations for a specific concentration relationship with Au NPs, which can be disturbed when the BL is switched off by a specific target, thereby changing the extent of large-scale aggregation. Large-scale aggregation can reduce the dispersion of Au NPs in the system, which causes a color-fade signal, unlike color changes such as red shift in other colorimetric assays. [33, 34] Large-scale aggregation is formed by a specific quantitative relationship between Au NP and BL. Figure II-1 shows the REVC at which aggregation occurs when BL is added to a specific amount of functionalized Au NP; this allows visual distinction. This can be explained as follows. First, when the amount of BL is small (region 1), the scale of the aggregation is small and visually discernible color changes do not occur, even if partial aggregation occurs. When the amount of BL increases, there is an aggregation region (region 2) that can be clearly distinguished visually. However, at a certain BL level beyond REVC (Region 3), excessive BL cannot induce the large-scale aggregation of Au NPs because the bridging of functionalized Au NPs is prevented; thus, no color change occurs. As shown in Figure II-1, when using a specific target that can change the effective

quantitative relationship between BL and functionalized Au NP inducing large-scale aggregation, REVC shifts to a higher BL concentration region. Since the amount of BL consumed depends on the concentration of the target, it is possible to detect *Salmonella* quantitatively by the extent of the REVC shift. Based on this principle, BL-based immunoassay can visually detect *Salmonella* sensitively.

II-3-2. Optimization of the conditions for the BL-based immunoassay

To develop an BL-based immunoassay for detecting *Salmonella*, it was necessary to optimize the BL concentration, the reaction time for creating large-scale aggregates, and the BL selectivity.

II-3-2.1. The range of BL concentration

Unlike conventional assays, which rely mainly on color changes caused by Au NP aggregation, this BL-based assay used the REVC, which was determined based on the quantitative correlation among nanoparticles, BLs, and the target. I use a fixed concentration of Au NPs to maintain a constant color. Therefore, the REVC shift was determined only by the quantitative relationship between the BLs and target pathogen concentrations. To evaluate the degree of the shift in REVC caused by the target, it was first necessary to determine the REVC with only the Au NPs and BLs as controls. The REVC was observed in the range of BL concentrations from 14 to 30 μg/mL (Figure II-S1). However, the inclusion of *Salmonella* (10^3) in the buffer made the

REVC shift to concentrations between 24 and 38 µg/mL, and the degree of the shift varied with the target (*Salmonella*) concentration in a non-linear manner. BL concentrations of 16, 18, 20, 36, 38, and 40 µg/mL were selected from repeated empirical results using concentrations of *Salmonella* ranging from 10 to 10^6 CFU/mL (data not shown); these BL concentrations clearly showed the REVC shift caused by the target concentration at the low and high ends.

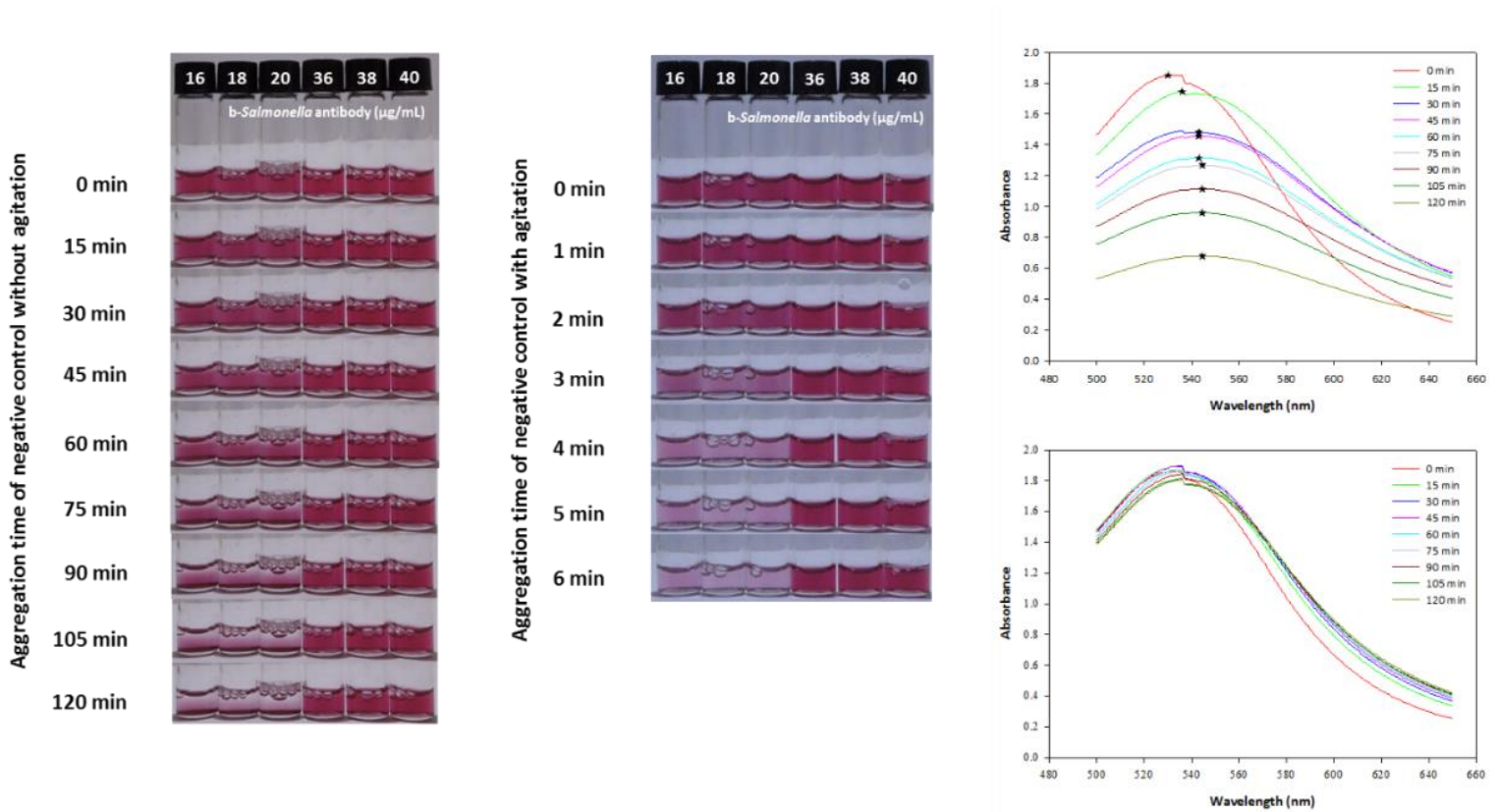

Figure II-2. Effect of REVC forming time in the negative control using aggregation with various concentrations of biotinylated *Salmonella* antibody as BLs and st-Au NPs. The color of the colloidal suspensions (a) without and (b) with agitation. Absorbance of UV-Vis spectra at SL concentrations of (c) 18 and (d) 38 μg/mL without agitation. ★ indicates the peak point.

II-3-2.2. The reaction time for creating large-scale aggregates

In the proposed assay, the total detection time depends on the time required for large-scale aggregation in the second testing step. When the test was performed with no agitation, it was possible to recognize color changes within 15 min; however, nearly 2 h were required for full precipitation (Figure II-2a). With agitation, however, a color change could be perceived after 1 min, and full precipitation occurred within 4 min (Figure II-2b).

Figures II-2c and d show the changes in wavelength and absorbance over time at BL concentrations of 18 and 38 μg/mL, respectively. The Au NP aggregates formed instantaneously after adding the Au NPs. The mean size of the Au NP aggregates is determined mainly by the relative concentrations of BLs and Au NPs, which affects the precipitation time. At 15 min, it was possible to recognize the slight color change caused by the increased size of the Au NP aggregates. The wavelength peak shifted to higher values (from 531.5 to 541.5 nm), and the curve pattern also changed. After 15 min, the REVC gradually appeared as the Au NP aggregates settled; the absorbance decreased as time passed. Therefore, the color clearance effect caused by the precipitation of Au NP aggregates could be distinguished after about 45 min, and the aggregates were all deposited after 120 min.

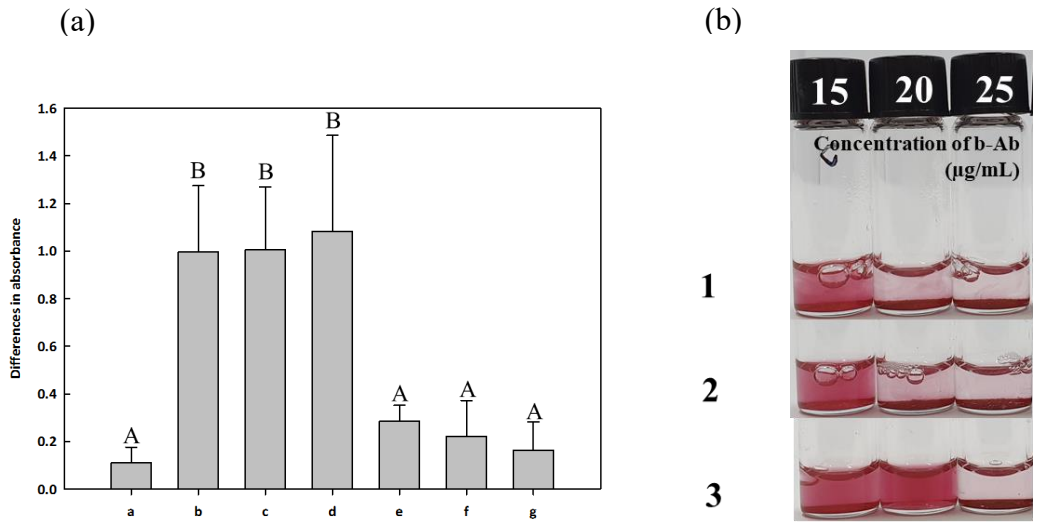

Figure II-3. Selectivity test. (a) Selectivity of the SL-based immunoassay for the detection of six model bacteria: **a**. negative control, **b.** *Salmonella* Typhimurium, **c**. *S.* Javiana, **d**. *S.* Newport, **e**. *Staphylococcus aureus*, **f**. *Escherichia coli* K-12 MG1655, and **g**. *E. coli* DH5α. (b) Selectivity of the BL-based immunoassay for the detection of three model bacteria in tomato sample: **1**. negative control, **2.** *E. coli* K-12 MG1655, *Staphylococcus aureus*, **3**. *E. coli* K-12 MG1655, *Staphylococcus aureus*, *Salmonella* Typhimurium. The concentrations of bacterial cells were all 10^5 CFU/mL. The error bars are the standard deviations of three repeat measurements. The different capital letters in the table indicate significantly ($p < 0.05$) different results as measured by Duncan's test.

II-3-2.3. Selectivity

Selectivity is also an important factor in the effectiveness of the assay. The selectivity of the b-Ab used in this assay was investigated using bacterial controls including *Salmonella* Typhimurium, *S*. Newport, *S*. Javiana, *Staphylococcus aureus*, *E*. *coli* K-12 MG1655, and *E*. *coli* DH5α. The bacterial concentration was maintained at 10^5 CFU/mL. The experimental results (Figure II-3 (a)) clearly showed that the differences in the absorbance of the other bacteria are much lower than those of the *Salmonella* group. The groups of *Salmonella* showed differences in the absorbance signal intensity of approximately 1.0, at which point it was possible to distinguish the color change with the naked eye. However, the other groups were not significantly different in terms of the signal intensity. This showed that b-Ab performed as a highly selective BL in this assay system. In addition, selectivity test was performed in tomato The experiment was performed from the following three groups:

1: only tomato sample (negative control)

2: tomato sample + E. coli K-12 MG1655, Staphylococcus aureus

3: tomato sample + E. coli K-12 MG1655, Staphylococcus aureus, Salmonella Typhimurium

The REVC shift was observed in group 3. This results show that this assay has selectivity for *Salmonella* in tomato.

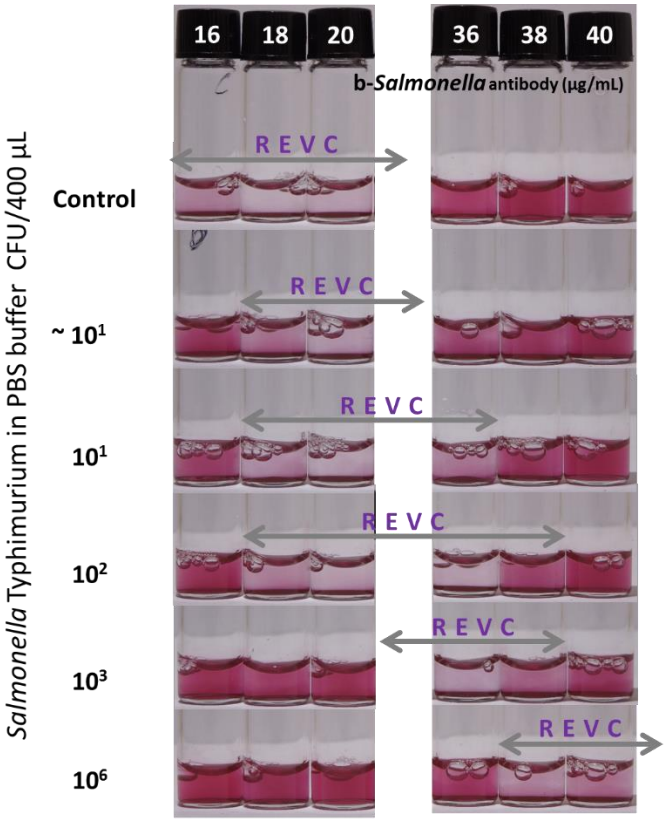

Figure II-4. Shift in REVC 2 h after performing the BL-based immunoassay for detecting *S.* Typhimurium (0, <10, 10, 10^2, 10^3, and 10^6 CFU/400 µL) using a fixed concentration of st-Au NPs (absorption: 0.43 @ 531.5 nm for the sample with 10 CFU/400 µL).

II-3-3. Detection of *Salmonella* using the BL-based immunoassay

Using the optimized conditions described above, the ability of the BL-based immunoassay to detect *Salmonella* in PBS was tested. Assays were performed using six concentrations of *Salmonella*: 0 (negative control), <10, 10, 10^2, 10^3, and 10^6 CFU/400 µL (positive control) in PBS. As shown in Figure II-4, the span of the REVC in the negative control samples appeared at BL concentrations of 16, 18, and 20 µg/mL. As the concentration of *Salmonella* increased from 0 to 10^6 CFU/400 µL, the span of the REVC also shifted to higher concentrations of BLs. Although the span of the REVC did not increase linearly, it was nevertheless possible to detect *Salmonella* quantitatively because the shift in REVC depended on the quantitative correlation between *Salmonella* and b-Ab. This immunoassay for *Salmonella* was extremely sensitive; it could distinguish *Salmonella* at <10, 10, 10^2, and 10^3 CFU/400 µL. The LOD of this assay was found to be <10 CFU/400 µL of *Salmonella* in PBS, as evaluated by the naked eye after a 45-min reaction without agitation; the first step took about 30 min, and after the second step, it was possible to recognize the color change after 15 min without agitation.

Several commercial biosensors are available. A lateral flow assay-based biosensor produced by DuPont (Wilmington, DE) can detect 1 CFU/assay of *Salmonella* within 15 min using antibodies, but it requires 8 h for enrichment. A rapid assay by Creative Diagnostics (Shirley, NY) can detect *Salmonella* within 10 min;

however, it has low sensitivity, with an LOD of 10^4 cells/mL. [35] Our rapid, highly sensitive BL-based immunoassay improves upon the limitations of these other assays.

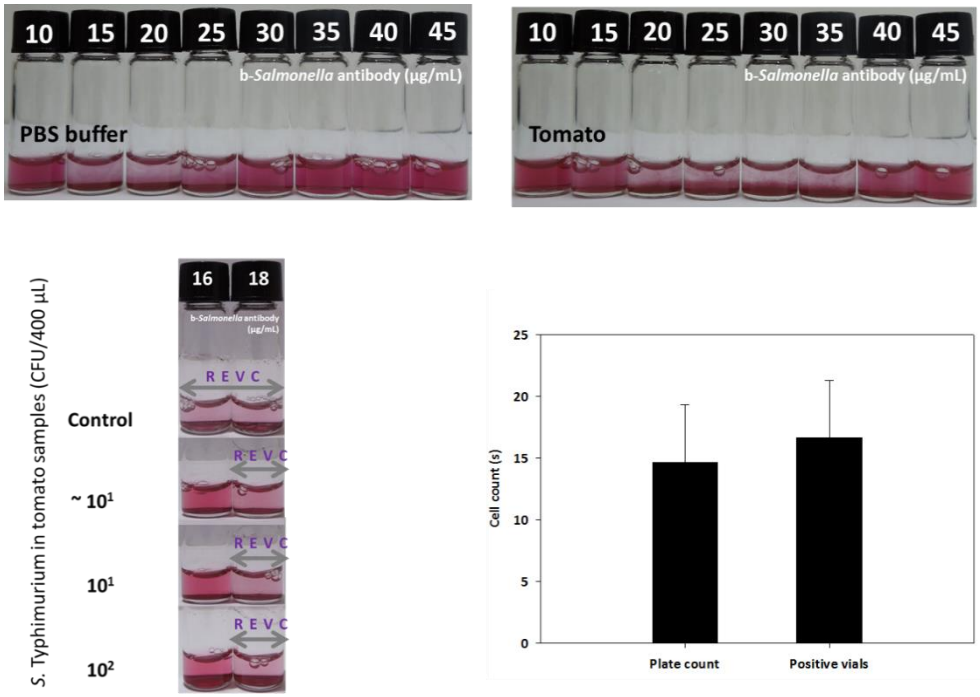

Figure II-5. Application of the BL-based immunoassay to the detection of S. Typhimurium. REVC of the control in PBS buffer and tomatoes in SL concentrations of 10–45 μg/mL. The REVC appears at SL concentrations of 15–25 and 20–35 μg/mL in (a) the PBS buffer and (b) tomatoes, respectively. (c) The REVC shift after performing the BL-based immunoassay for on-site detection of *S.* Typhimurium (0, <10, 10, and 10^2 CFU/mL) in fresh tomato samples. (d) Results of single bacterial cell detection. The number of bacterial cells was determined by a plate count and the BL-based immunoassay. The mean numbers of bacteria were 14.6 and 16.7 in plate-count and BL-based immunoassays, respectively. The two assays had a strong correlation ($R^2 = 0.80$).

II-3-4. The use of an BL-based assay with contaminated tomato samples

The detection of pathogens in food has some difficulties, not only because of the wide range in pH but also because many of the nutritional contents can affect the biosensor signals. However, BL-based immunoassays can establish a base control for each food sample so that only the pathogen causes the REVC shift. Based on this concept, pathogens can be detected using the difference in REVC from pathogen-free controls. The result is extremely powerful for detecting *Salmonella* on diverse foods, including tomatoes. Comparing the control tomato samples with PBS buffer, the REVCs were 15–25 and 20–35 μg/mL BL for PBS buffer and tomato, respectively (Figures II-5a and II-5b). Therefore, when a base control is available, the BL-based immunoassay can detect *Salmonella* at commercial tomato processing sites, unlike other biosensors, which are limited by the effects of the food composition. [36] Furthermore, the BL-based immunoassay uses the large-scale aggregation of Au NPs to make the color, and it is not affected by the natural color of tomatoes.

Many food safety agencies, such as the Food and Drug Administration, have established a zero-tolerance policy for *Salmonella* in ready-to-eat foods, including fresh produce (FDA 2009). This means that *Salmonella* detection in fresh produce should be very sensitive. Furthermore, to test directly at industrial sites, the test method must be simple, fast, and easy to handle. For this reason, the range of BL concentrations should be set simply and sensitively. Therefore, the low end (16 and 18 μg/mL of BL) of the control REVC in Figure II-4 was selected when detecting

Salmonella in tomatoes using the BL-based immunoassay; the REVC shifted sensitively in this concentration range even when there was a low concentration ($<10^1$ CFU/400 μL) of *Salmonella*. BL-based immunoassays have very strong sensitivity for the detection of bacteria. Because a single bacterium has a relatively high number of antigens, even low concentrations of bacteria can take up a considerable amount of BL. Thus, REVC shift can easily occur since the effective concentration relationship between st-Au NP and BL is disturbed.

The REVC of the samples with *Salmonella* shifted to 18 μg/mL, differing from the control (Figure II-5c). Even concentrations as low as <10 CFU/400 μL were clearly detected. The <10 CFU/400 μL concentration correspond to 10 cells/g for fresh tomato products. Tomatoes are often cross-contaminated with small amounts of *Salmonella*, but the bacteria increase rapidly at room temperature during transportation or when on display in retail shops. [6] Therefore, low-level detection of *Salmonella* is very important when harvesting or processing tomatoes.

To confirm the actual *Salmonella* concentrations in <10 CFU/400 μL samples, a verification experiment using a single-cell detection method was carried out. To examine whether BL-based immunoassay can detect a single bacterial cell, a *Salmonella* Typhimurium suspension was serially diluted and plate counted. The resulting 1.0-OD_{600} suspension appeared to contain 9.7×10^7 CFU/mL. Approximately 10 cells (based on optical density) were confirmed by plate counting and BL-based immunoassay. The suspension containing about 10 bacterial cells was divided into 30

independent vials. Each vial was analyzed by BL-based immunoassay and the vials showing the REVC shift were counted (see Figure II-S2). In three independent assays, the numbers of cells counted using the BL-based immunoassay and plate-count method were 14 *vs.* 12.33, 22 *vs.* 19.33, and 14 *vs.* 12, respectively. The R^2 for the results of the two methods was 0.80. The mean and standard deviation are plotted in Figure II-5d. This showed that the BL-based immunoassay method was sensitive to <10 CFU/400 μL of *Salmonella* with an LOD of 10 CFU/g of tomato sample, as evaluated by the naked eye after a 45-min reaction with agitation. Therefore, the BL-based immunoassay shows that it is possible to detect pathogens such as *Salmonella* in the field of the fresh produce industry where the detection of low pathogen concentrations is required.

II-4. References

1. X. Guo, M. W. van Iersel, J. Chen, R. E. Brackett and L. R. Beuchat, *Applied and Environmental Microbiology*, 2002, 68, 3639-3643.
2. J. Heaton and K. Jones, *Journal of applied microbiology*, 2008, 104, 613-626.
3. C. Hedberg, F. Angulo, K. White, C. Langkop, W. Schell, M. Stobierski, A. Schuchat, J. Besser, S. Dietrich and L. Helsel, *Epidemiology & Infection*, 1999, 122, 385-393.
4. M. Lynch, R. Tauxe and C. Hedberg, *Epidemiology and infection*, 2009, 137, 307-315.
5. A. N. Olaimat and R. A. Holley, *Food microbiology*, 2012, 32, 1-19.
6. I. B. Hanning, J. Nutt and S. C. Ricke, *Foodborne Pathogens and Disease*, 2009, 6, 635-648.
7. R. Zhuang, L. Beuchat and F. Angulo, *Applied and Environmental Microbiology*, 1995, 61, 2127-2131.
8. M. I. Gil, M. V. Selma, F. López-Gálvez and A. Allende, *International journal of food microbiology*, 2009, 134, 37-45.
9. M. S. Islam, T. Matsui and Y. Yoshida, *Scientia Horticulturae*, 1996, 65, 125-136.
10. P. Mäkelä, J. Kärkkäinen and S. Somersalo, *Biologia Plantarum*, 2000, 43, 471-475.
11. S. Römer, P. D. Fraser, J. W. Kiano, C. A. Shipton, N. Misawa, W. Schuch and P. M. Bramley, *Nature biotechnology*, 2000, 18, 666-669.
12. B. Van Dorst, J. Mehta, K. Bekaert, E. Rouah-Martin, W. De Coen, P. Dubruel, R. Blust and J. Robbens, *Biosensors and Bioelectronics*, 2010, 26, 1178-1194.
13. B. Pérez-López and A. Merkoçi, *Trends in Food Science & Technology*, 2011, 22, 625-639.
14. P. Barrow, A. Berchieri Jr and O. Al-Haddad, *Avian diseases*, 1992, 227-236.
15. L. Croci, E. Delibato, G. Volpe, D. De Medici and G. Palleschi, *Applied and environmental microbiology*, 2004, 70, 1393-1396.
16. S. Flint and N. Hartley, *Letters in applied microbiology*, 1993, 17, 4-6.
17. B. Malorny, E. Paccassoni, P. Fach, C. Bunge, A. Martin and R. Helmuth, *Applied and environmental microbiology*, 2004, 70, 7046-7052.
18. K. Rahn, S. De Grandis, R. Clarke, S. McEwen, J. Galan, C. Ginocchio, R. Curtiss and C. Gyles, *Molecular and cellular probes*, 1992, 6, 271-279.
19. Y.-C. Chiang, C.-Y. Yang, C. Li, Y.-C. Ho, C.-K. Lin and H.-Y. Tsen, *International journal of food microbiology*, 2006, 107, 131-137.
20. H.-Y. Tsen, S.-J. Wang, B. A. Roe and S. S. Green, *Applied microbiology and biotechnology*, 1991, 35, 339-347.
21. S. E. Hanna, C. J. Connor and H. H. Wang, *Journal of Food Science*, 2005, 70.

22. P. Leonard, S. Hearty, J. Brennan, L. Dunne, J. Quinn, T. Chakraborty and R. O'Kennedy, *Enzyme and Microbial Technology*, 2003, 32, 3-13.
23. K. Asplund and E. Nurmi, *International journal of food microbiology*, 1991, 13, 177-181.
24. R. Tauxe, H. Kruse, C. Hedberg, M. Potter, J. Madden and K. Wachsmuth, *Journal of Food Protection*, 1997, 60, 1400-1408.
25. L. R. Beuchat and J.-H. Ryu, *Emerging infectious diseases*, 1997, 3, 459.
26. X. Guo, J. Chen, R. E. Brackett and L. R. Beuchat, *Journal of food protection*, 2002, 65, 274-279.
27. X. Guo, J. Chen, L. R. Beuchat and R. E. Brackett, *Applied and environmental microbiology*, 2000, 66, 5248-5252.
28. S. Lim, O. K. Koo, Y. S. You, Y. E. Lee, M.-S. Kim, P.-S. Chang, D. H. Kang, J.-H. Yu, Y. J. Choi and S. Gunasekaran, *Scientific reports*, 2012, 2, 456.
29. E. Hauser and J. Lynn, *Industrial & Engineering Chemistry*, 1940, 32, 659-662.
30. M.-K. Park, J. W. Park, H. C. Wikle and B. A. Chin, *Journal of Biosensors and Bioelectronics*, 2012, 3, 1000113.
31. B. S. Mahmoud, *Food microbiology*, 2010, 27, 1057-1063.
32. Y.-C. Chang, C.-Y. Yang, R.-L. Sun, Y.-F. Cheng, W.-C. Kao and P.-C. Yang, *Scientific reports*, 2013, 3, 1863.
33. W. Zhao, M. A. Brook and Y. Li, *ChemBioChem*, 2008, 9, 2363-2371.
34. R. Elghanian, J. J. Storhoff, R. C. Mucic, R. L. Letsinger and C. A. Mirkin, *Science*, 1997, 277, 1078-1081.
35. S. M. Yoo and S. Y. Lee, *Trends in biotechnology*, 2016, 34, 7-25.
36. L. A. Terry, S. F. White and L. J. Tigwell, *Journal of agricultural and food chemistry*, 2005, 53, 1309-1316.

II-5. Appendix: Optimization of BL-based assay

II-5-1. Evaluation of the degree of shift in REVC

To evaluate the degree of shift in REVC caused by the target, it was first necessary to determine the REVC that naturally occurred with only the Au NPs and BLs as controls.

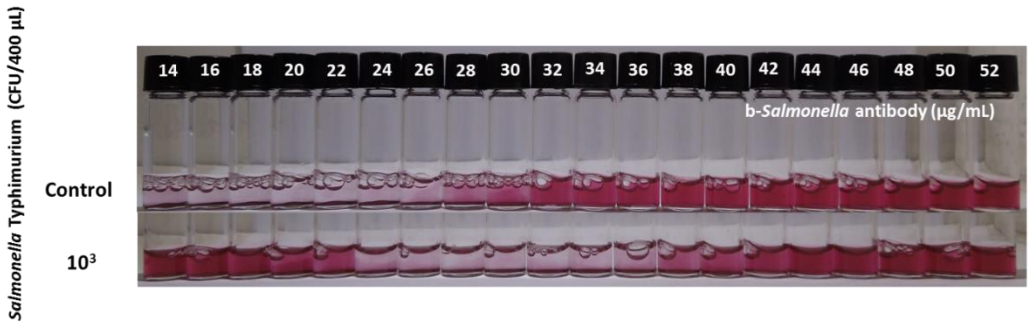

Figure II-S1. The visual signal results of the negative control and *S.* Typhimurium (10^3 CFU/400 μL) in BL concentrations of 14–52 μg/mL in PBS. In the control, the REVC was in BL concentrations of 14–30 μg/mL, whereas for *Salmonella* it appeared at concentrations of 24–38 μg/mL.

II-5-2. Detection of a single bacterium

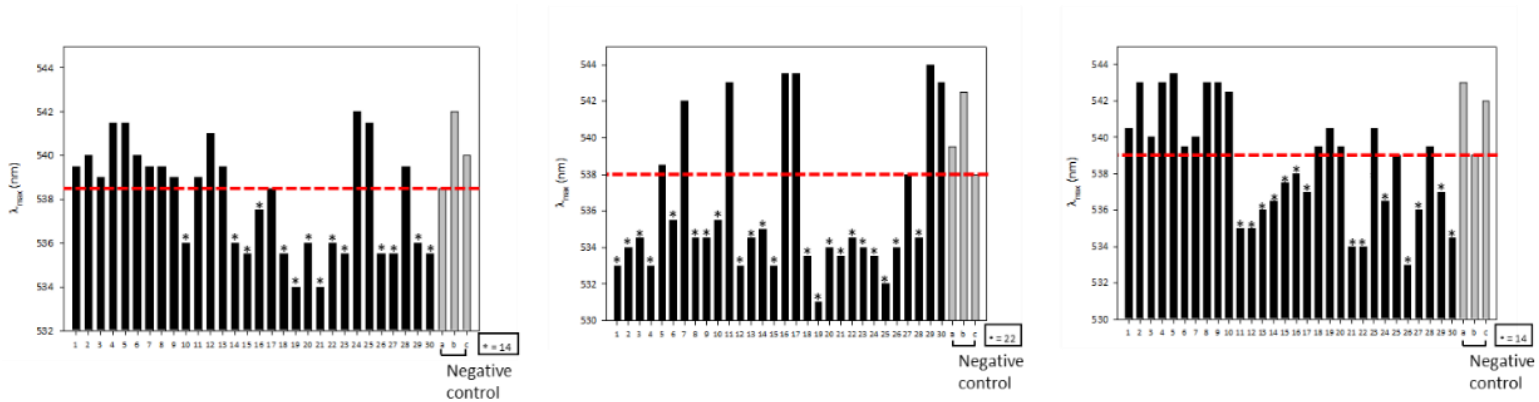

Figure II-S2. Detection of a single bacterium using BL-based immunoassay. Bacterial suspensions containing 10 bacterial cells, estimated based on OD_{600} values, were divided equally into 30 vials. Each sample followed the assay protocol. The λ_{max} of each sample was measured as above. Three independent assays were performed, with stars marking positive signal containing bacteria. The three gray bars on the right show the signals for negative controls, and dashed line indicates the lowest λ_{max} in the three controls. In three independent assays, 14, 22, and 14 positive vials were obtained.

II-5-3. Confirmation of the effectiveness of homogenization

To confirm the effectiveness of homogenization by hand, comparison of three homogenization methods was performed: mashing tomato by hand, stomaching without peptone water, and stomaching with peptone water (1:10 dilution). There were no statistically significant differences among the three experimental results.

Table II-S1. Comparison of homogenization methods

Homogenization method	Inoculation	Population (log CFU/mL)[b]	
		CFU/mL	CFU/tomato (SD)[c]
Hand-mashing	Control[a]	ND[d]	ND
	Treatment	7.48	9.78 (0.15) A
Stomaching without dilution buffer	Control	ND	ND
	Treatment	7.71	9.43 (0.18) A
Stomaching with dilution buffer	Control	ND	ND
	Treatment	7.54	9.84 (0.43) A

[a]Tomatoes were treated with 20 mL of ethanol (70%) for 1 min and then washed in 200 mL of DW for 5 min.
[b]Populations of Salmonella were analyzed for numbers (log CFU/mL) by direct plating; values were converted to log CFU per tomato (200 g). The mean population applied to each tomato by spot inoculation was 9.86 log CFU/mL.
[c]Mean values (log CFU per tomato) in columns were analyzed for significant differences. The letter next to SD value indicates not significantly different by Duncan test at $p < 0.05$: within mashing with hand and stomaching without dilution buffer.
[d]Not detected.

The crushing of a tomato was rated as follows:

0 = none

1 = cracks on tomato surface

2 = exposure of the internal structure

3 = segmentation of external structure

4 = no more dividing of external structure by hand

The homogenization was subjectively evaluated by applying manual pressure to tomatoes in a Stomacher Bag.

As a result, after step 4, the tomato was determined to be homogenized.

II-5-4. Quantification of Color Change by Precipitation

To objectively recognize the color change caused by the precipitation of Au NP aggregates, the degree of precipitation was evaluated both by visual observation and a spectrophotometer. As shown in Figure II-S1, the precipitation was observed every 10 minutes and the absorbance of the peak was traced at the same time. To quantify the color change due to precipitation, the absorbance equation A was defined as shown below, which is expressed as the decreasing absorbance ratio (%) at each time interval to that at 0 min.

$$A\ (\%) = (1-(A_t/A_0)) \times 100$$

A_t: absorbance in peak at time t

A_0: initial absorbance in peak at 0 min

The second reaction of the BL-based assay is twofold: the aggregate formation reaction and the aggregate precipitation reaction (a rate-limiting step). As the aggregates grow, the rate of aggregation decreases. When aggregates of a certain size are formed, these aggregates begin to precipitate. As shown in Figure II-S2, the color change due to precipitation was recognizable by the naked eye after about 40 min, and A was about 13% at this time.

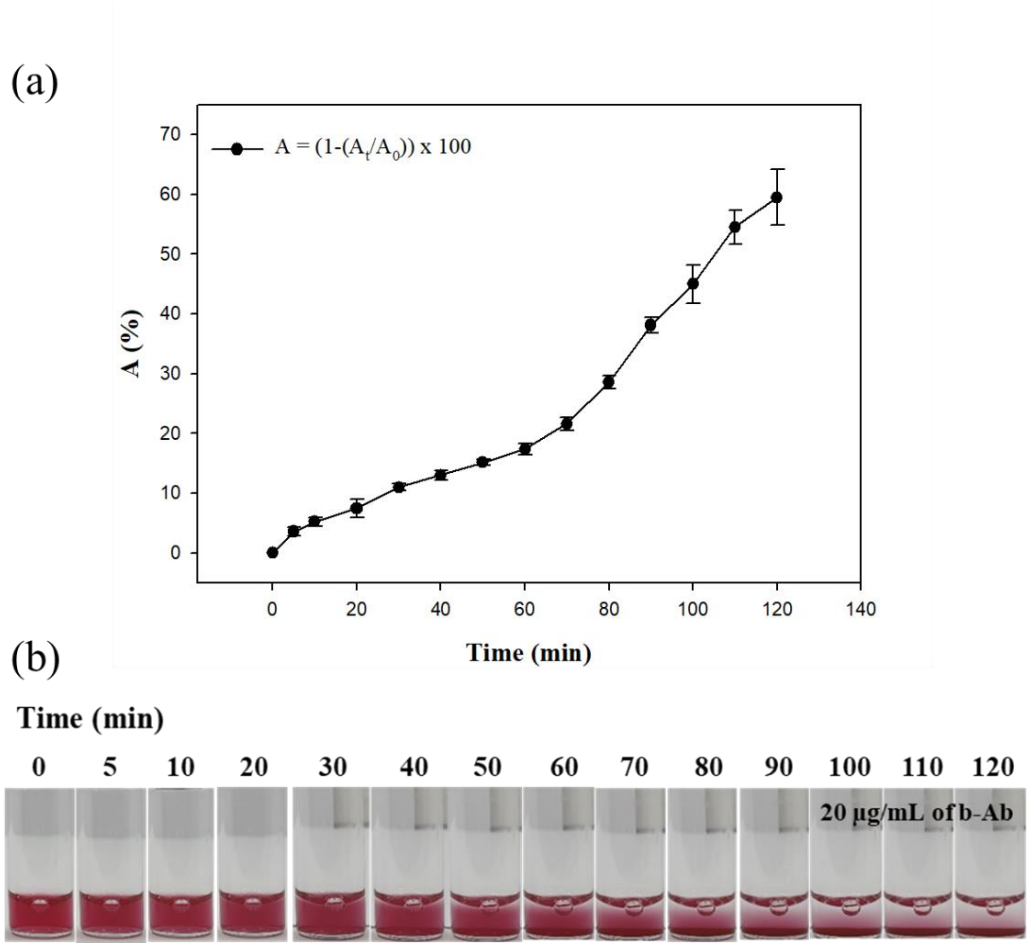

Figure II-S3. Quantification of color change by precipitation. Color changes of gold nano-aggregates by precipitation was tracked at 10-min intervals for 120 min by (a) a spectrophotometer to determine the absorbance A and (b) the naked eye.

Chapter III. Colorimetric bi-functional linker-based bioassay for ultrasensitive detection of prostate-specific antigen as a cancer biomarker

Published in the Analyst

(J. Hahn, E. Kim, Y. You, and Y. J. Choi, *Analyst.* 2019, 144, 4439-4446)

III-1. Introduction

The ultrasensitive detection of protein analytes is essential for food safety regulations and environmental monitoring, as well as medical diagnostics. [1-3] The important role of protein analyte detection in these fields has driven the steady increase in demand for exploiting simple, fast, cost-effective, selective, and highly sensitive biosensors. [4, 5] To date, various strategies based on different detection signal-switching principles have been utilized for protein detection, including electrochemiluminescence, fluorescence, chemiluminescence, quartz crystal microbalance, electrochemistry, and colorimetric methods. [6-13] Among the various protein detection methods, colorimetric detection is preferred for its use of the visible spectrum, easy use, simplicity, and rapid/direct readout with the naked eye. [14-16] Unfortunately, most developed colorimetric assays have poor sensitivity due to their use of weak and limited signal amplification strategies. [17, 18]

Colorimetric detection using gold nanoparticles (Au NPs) with unique optical properties, including local surface plasmon resonance (LSPR) absorption and resonance scattering, enables the quick detection of small molecules including protein biomarkers. [19-21] The use of Au NPs in biosensing has several advantages. This type of colorimetric detection can often be performed visually with the naked eye, enabling rapid, inexpensive, and portable detection. [22-24] However, the sensitivity of colorimetric methods that use Au NPs for protein analysis is no better than that of the conventional fluorescence colorimetric methods. [25] There are two reasons for this:

First, Au NPs bind to a relatively large number of targets, unlike fluorescent colorimetric methods in which one target binds to one chromogenic reagent. Second, Au NP aggregates often have very low absorbance compared to dispersed Au NPs. Therefore, the development of colorimetric sensors that use Au NPs and have high sensitivity is an important goal for many researchers.

Prostate-specific antigen (PSA), which is detectable in human serum, is a useful biomarker for diagnosing prostate and breast cancers. In general, a total PSA value of 2.5 ng/mL is a highly probable indication of prostate cancer. [26] It is therefore important to detect this PSA level and diagnose this cancer early. After treatment, it is necessary to prevent the recurrence of this disease by monitoring the PSA in human serum. [27] Although PSA is the most useful cancer marker for the diagnosis and management of prostate cancer, many studies have also found a concentration of free PSA at a much lower level (1000 times lower than male) in female sera, mainly in the breast and secretions. [28, 29] PSA is produced in the majority of breast tumors and may be a good prognostic indicator of breast cancer. For these reasons, it is very important to detect PSA at very low concentrations during prostate and breast cancer screenings and diagnoses. [30,31]

Several studies have introduced an aggregation system of Au NPs using bi-functional linkers (BLs), which amplify the visible signal to improve sensitivity. [32-34] The BL-based aggregation mechanism enables visual signal amplification by inducing the large-scale aggregation of nanoparticles. In addition, BL features a

unique property: the independence of the target recognition and visual signal generation processes. In this study, I designed an experiment to control the reaction surface area of Au NPs by controlling their concentration in the BL aggregation system, thereby providing high sensitivity without reducing the color signal intensity. Thus, representative cancer biomarkers, i.e., prostate-specific antigens, can be detected more quickly and sensitively.

.

III-2. Materials and Methods

III-2-1. Chemicals, reagents, and instruments

I purchased bovine serum albumin (BSA), 1-mM tetrachloroaurate, phosphate-buffered saline (PBS), tween 20, 3,3',5,5'-tetramethylbenzidine (TMB), streptavidin coated horseradish peroxidase (HRP) and streptavidin from Sigma-Aldrich (Madison, WI), and tetraborate pH standard solution from Wako Pure Chemicals (Osaka, Japan). I purchased anti-PSA antibody (biotin) from Abcam (Cambridge, MA) and trisodium citrate, sulfuric acid, sodium vials, and ethanol from local suppliers.

The buffer I used for Au NP synthesis was sterilized distilled water (1), which I prepared with 1% (w/v) trisodium citrate as a reducing agent. The buffers used for the BL-based immunoassay were 0.01 mol/L PBS (pH 7.4) prepared with 0.5% (w/v) BSA for blocking, and 0.01 mol/L tetraborate pH standard solution (pH 7.4) for diluting streptavidin.

I performed the BL-based immunoassay in glass vials (4science, South Korea). To determine the assay absorbance, I used a UV-1700 spectrophotometer (Shimadzu, Japan).

I performed the ELISA in 96-well (4science, South Korea). To determine the assay absorbance at 450 nm, I used Multiskan GO microplate spectrophotometer (Thermo Scientific, FL).

III-2.2. Nanoparticle fabrication

I prepared colloidal gold particles 13 nm in size by reducing tetrachloroaurate with trisodium citrate, as described by Hayser and Lynn. [35] I heated fifty milliliters of 1 mM tetrachloroaurate solution while continuously stirring. When the solution began to boil, I quickly added 5 mL of 1% (w/v) trisodium citrate to the sample, and heated the solution until it turned a reddish purple. When there was no further color change, I slowly cooled the solution at 50 °C for 30 min.

III-2.3. Au NP surface functionalization

To functionalize the Au NPs (12.36 nm in diameter), I coated 200 μL of 0.2 mg/mL streptavidin dissolved in a tetraborate solution with a pH of 7.4 onto 600 μL of Au NPs, having an absorbance of 0.4 (1/10 dilution) at 520 nm, and then washed them using centrifugation at 10,000 g to remove any unbound streptavidin. [36, 37] These Au NPs functionalized with streptavidin molecules (st-Au NPs) showed a peak at 531.5±0.5 nm. The peak spectra of the Au NP dispersions before and after nanoparticle functionalization shift by about 10 nm, which means that streptavidin was effectively adsorbed on the Au NP surface and changed the effective thickness of the layer (spectral shift).[38] I estimated the concentration of Au NPs in solution based on peak absorbance values of 0.185, 0.2, 0.37, and 0.74 for 1/10 dilution samples on

the UV-Vis spectra, respectively. I mixed the st-Au NPs with 0.1% (w/v) BSA dissolved in PBS as a blocking and dilution buffer.

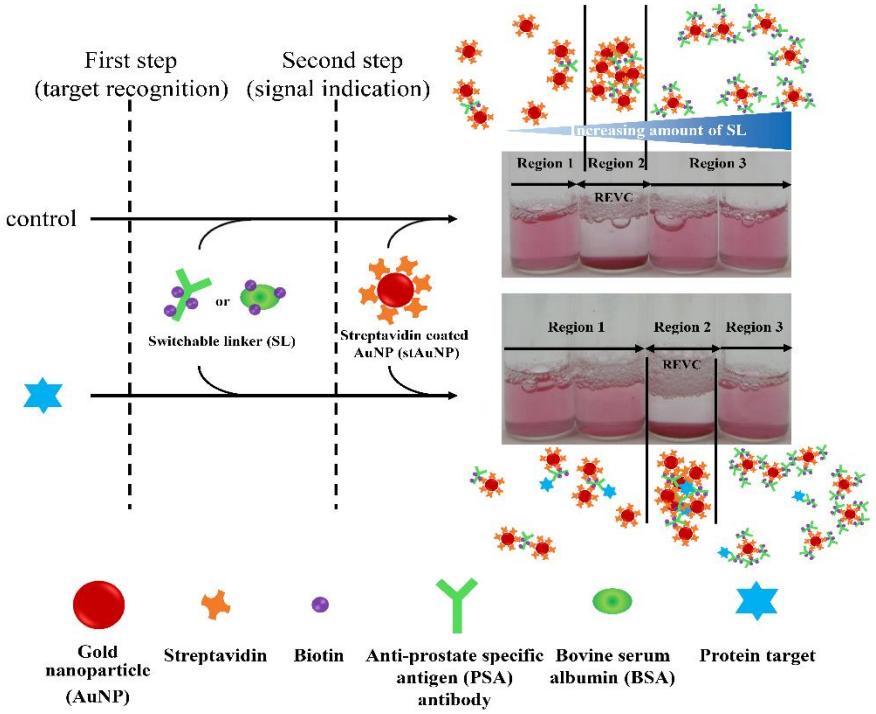

Figure III-1. Schematic representation of an BL-based assay. First, the biotinylated antibody or BSA as BL was either added or not added to the target. Then, functionalized nanoparticles (st-Au NPs) were added to the solutions

III-2.4. Detection of streptavidin and PSA using BL-based assay

In this assay, I used biotinylated BSA (b-BSA) and biotinylated anti-prostate specific antigen antibody (b-Ab), which was the BL, for the detection of streptavidin and PSA, respectively. Figure. III-1 shows a schematic representation of an BL-based assay, which I performed in a total reaction volume of 200 μL, containing 100 μL of st-Au NP solution (absorbance of 2 at 531.5 nm) at a fixed concentration, 50 μL of BLs, and 50 μL of a test sample (either PBS at pH 7.4 or serum at pH 7.35). First, I mixed 50 μL of the test sample with 50 μL of the BLs at various concentrations (10 μg/mL, 15 μg/mL, 20 μg/mL, 25 μg/mL, and 30 μg/mL in the case of both b-BSA and b-Ab). After an appropriate reaction time (> 30 min) without stirring, I added 100 μL of st-Au NPs to the mixture and allowed the sample to stand for 2 h. To determine the quantitative correlation among the targets in the samples, BLs, and st-Au NPs, I monitored a range of linker concentrations exhibiting visual color change (REVC).

III-2.5. Selectivity of b-antibody as a bi-functional linker.

To determine the selectivity of the BLs-based assay, I exposed b-Ab to three different proteins at concentrations of 10 ng/mL: ovalbumin, streptavidin, and human serum albumin. I added b-Ab (25 μg/mL) to the following five solutions: a control (nonexistence of target, PBS), and solutions of ovalbumin, streptavidin, HAS, and PSA (10 ng/mL). After 30 min, I added st-Au NPs to each sample. 120 min after the addition of st-Au NPs, I measured the maximum absorbance of the mixture with a

UV-Vis spectrophotometer and calculated the difference in absorbance between the two points (control and each sample).

III-2.6. Enzyme-Linked Immunosorbent Assay (ELISA)

The PSA was diluted to various concentrations (0.2, 0.5, 1.0, 2.0, 4.0 6.0 8.0 10, 20, 40, 60, 80, and 100 ng/mL) in human serum. One hundred microliter aliquots of each PSA dilution was incubated overnight at 4 ° C in individual wells of a 96-well plate. Afterwards, wells were thoroughly washed 3 times with 200 μL of 0.05% PBS-Tween. To block the remaining protein-binding sites in the coated wells, 200 μL of blocking solution (1% BSA in PBS) was added to each well, and the plate was incubated for 2 h at room temperature. The wells were again thoroughly washed 3 times with 200 μL of PBS+0.05% Tween. One hundred microliters of biotinylated human PSA antibody, diluted to 1.0 μg/mL in dilution buffer (0.1% BSA in PBS) immediately before use, was added to each well and incubated for 2 h at room temperature. Wells were again thoroughly washed 3 times with 200 μL of PBS-Tween 0.05 %, again. One hundred microliters of streptavidin conjugated HRP was added to each well and the plate was incubated for 1 h at room temperature. Afterwards, plates were thoroughly washed 3 times with 200 μL of PBS-Tween 0.05 %. One hundred microliters of TMB solution was added, and the plate was incubated until sufficient color developed. The reaction was stopped with 100 μL of 2M sulfuric acid per well. I measured maximum absorbance of each well at 450 nm with a Multiskan GO

microplate spectrophotometer.

III-2.7. Statistical analysis

The data represent an average of at least three independent experiments or measurements.

III-3. Results and Discussion

III-3-1. BL-based assay scheme: characteristics of the BL and its construction

The BL, which is the core of this system, should satisfy three conditions. First, it should crosslink the nanoparticles; secondly, it should be able to bind to the analyte; and lastly, when combined with the analyte, the system's ability to crosslink the nanoparticles should be constrained. I refer to this situation as the linker being switched-off. When this linker is switched off by the target, two phenomena happen, as follows. First, the quantitative relationship between the linker and the Au NPs changes. Second, as the relationship changes, the range of REVC linker concentrations shift to the direction of high linker concentrations. Therefore, BL-based assays can detect targets visually and semi-quantitatively. In this study, I used b-BSA and b-Ab as BLs to detect streptavidin and PSA, respectively. I designed an BL-based assay using stAu NPs, with b-BSA and b-Ab serving as BLs to detect streptavidin and PSA, respectively, as the protein analytes.

As shown in Figure III-1, an BL-based assay should be designed in two sequential steps: (Step 1) adding the BLs (i.e., b-BSA and b-Abs) to the sample, which is the target recognition step, followed by (Step 2), the addition of the stAu NPs, which is the signal indication step. In this experiment, the total reaction volume was 200 μL, comprising 100 μL of stAu NP colloid solution at a fixed concentration, 50 μL of the BLs at various concentrations, and 50 μL of the test samples. After allowing the

linker-target reactions to occur for about 30 min with shaking, I added st-Au NPs to the mixture, and allowed it to stand for an additional 2 h. The color change, which is the signal indication, occurs according to the quantitative correlation among the st-Au NPs, BLs, and targets in the test system.

After the above reaction, I can represent the results by three regions: regions 1 and 3, in which no aggregates precipitated because the number of linkers to react with the particle is insufficient (region 1) or is the binding site of the particle is already full with the linker (region 3), and region 2, in which sedimentation occurs and is observable as a color change, known as REVC. I determined the REVC of the negative control samples by the quantitative relationship between the st-Au NPs and BLs. In samples containing the target substances streptavidin and PSA, partial BLs bind to the target material and change the concentration range of the BLs to that in which REVC occurs. Therefore, a sample containing the target substance, when compared to the control sample, will exhibit REVC at a higher concentration range. This color difference can be used to quantitatively detect the target.

In the PSA–antibody and streptavidin–biotin cases, the equilibrium dissociation constants (K_D) are known to be roughly 10^{-12}/M and 10^{-15}/M, respectively, and the reactions of these two steps show different degrees of susceptibility. [39, 40] However, the difference in the dynamics of these two reactions does not affect the system operation, which can be explained as follows: First, the system consists of two independent, sequential steps. Second, each reaction occurs at a different binding site

and has a minimal effect on the other reaction, and they are not competitive. Third, the streptavidin–biotin reaction occurs much more rapidly than the PSA–antibody reaction, resulting in the rapid formation of large-scale aggregates of Au NP with BL. These large-scale aggregates will be precipitated by gravity depending on their size, which results in the visual signal. In this situation, even if the BL (i.e., the BL detached from the PSA) is switched on by the reverse reaction of PSA–BL it has very little chance of reacting with the aggregates. This is because the larger are the aggregates, the relatively slower is the reaction rate. Au NPs that did not participate in the formation of aggregates could bind with the switched-on BL, but this would generate relatively small-scale aggregates that cannot be precipitated and would be very unlikely to affect the REVC.

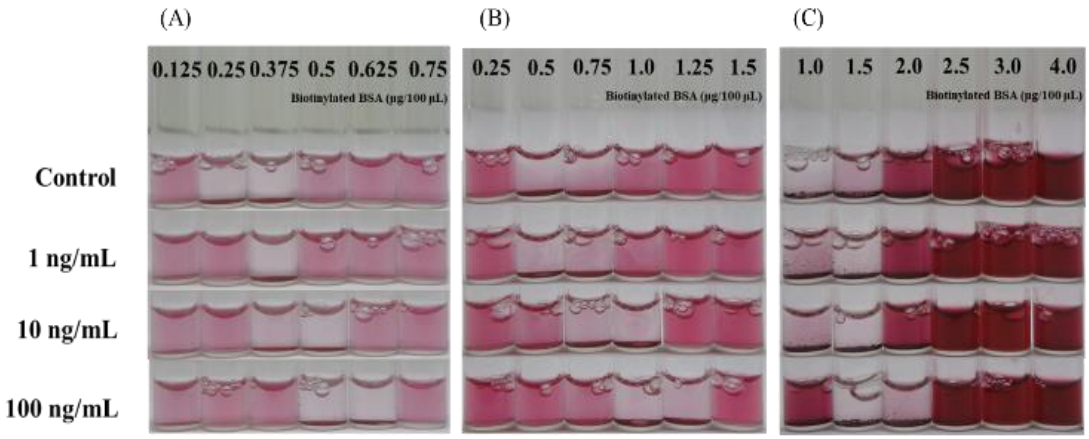

Figure III-2. Difference in sensitivities of three concentrations of Au NPs to the BL-based assay using three concentrations of streptavidin (1 ng/mL, 10 ng/mL, and 100 ng/mL) as the model target. The three Au NP concentrations showed peak absorbance values of (A) 0.185, (B) 0.37, and (C) 0.74 for 1/10 dilution samples, respectively.

III-3.2. Determination of the concentration of Au NPs

I determined the concentration of Au NPs to identify protein targets with high sensitivity. Previous studies of BL-based assay have shown signal recognition to be an independent process that occurs by changing the REVC without directly inducing the aggregation of Au NPs. [33] This indicates two features of the BL-based assay: first, the signal is amplified by the presence of sediments of large-scale aggregates of Au NPs, and not by a simple color change; second, the BL-based assay is not affected by the type and size of the targets during the signal recognition process. In particular, the lower the concentration of Au NPs, the lower the total surface area of Au NPs and the lower the concentration of linkers required for large-scale aggregation. When the linker is switched off by the target, the correlation between the Au NP and the linker causing large-scale aggregation is reestablished. Therefore, I hypothesized the lower the concentration of the linker, the more the REVC could be shifted by a small amount of the target. There are several strategies to control the sensitivity of the BL system such as controlling the size and surface load of nanoparticle, but the simplest and most effective way is to control the concentration of the particles. In this study, I designed the experiment by adjusting the total concentration of Au NPs in order to control the total reaction surface area by the simplest method. However, with respect to the concentration of the particles, the lower the concentration, the weaker the color, and the higher the concentration, the lower the colloid stability of the particles. Therefore, there is an appropriate range of concentrations for this assay. Based on the results of

number of experiments, I analyzed the sensitivity of the BL-based assay using three Au NP concentrations (peak absorbance values of 0.185, 0.37, and 0.74 at 1/10 dilution) (Figure III-2). These concentrations of Au NPs in solution were estimated based on the absorbance value as ~4.94×10^{12}, ~9.88×10^{12}, and ~1.98×10^{13} particles/mL, in the low order. [39] The results revealed that as the concentration of Au NPs decreased, REVC shifting occurs more sensitively. Low concentrations of Au NPs mean that the total surface area of Au NPs that can react with the linkers is small. The smaller the total surface area involved in the reaction, the better is the sensitivity due to the occurrence of the switching-off phenomenon with a smaller concentration of targets. In addition, the REVCs in the control samples of each concentration were 0.25 μg/mL and 0.375 μg/mL, 0.5 μg/mL and 1.0 μg/mL, and 1.0 μg/mL and 2.0 μg/mL at peak absorbances of 0.185, 0.37, and 0.74 for 1/10 dilute solutions, respectively. As the concentration of Au NPs doubled, the REVC in the control samples appeared to increase to exactly twice the linker concentration. This indicates that there is a quantitative correlation between Au NP and the linker in the formation of large aggregates for sedimentation. Finally, using absorbance as a measure of concentration, I chose an Au NPs concentration of 2 for use in this study, taking into account the visually distinct concentrations and sensitivities. Therefore, the sensitivity of BL-based assays can be improved by changing the quantitative relationship between Au NP and BL.

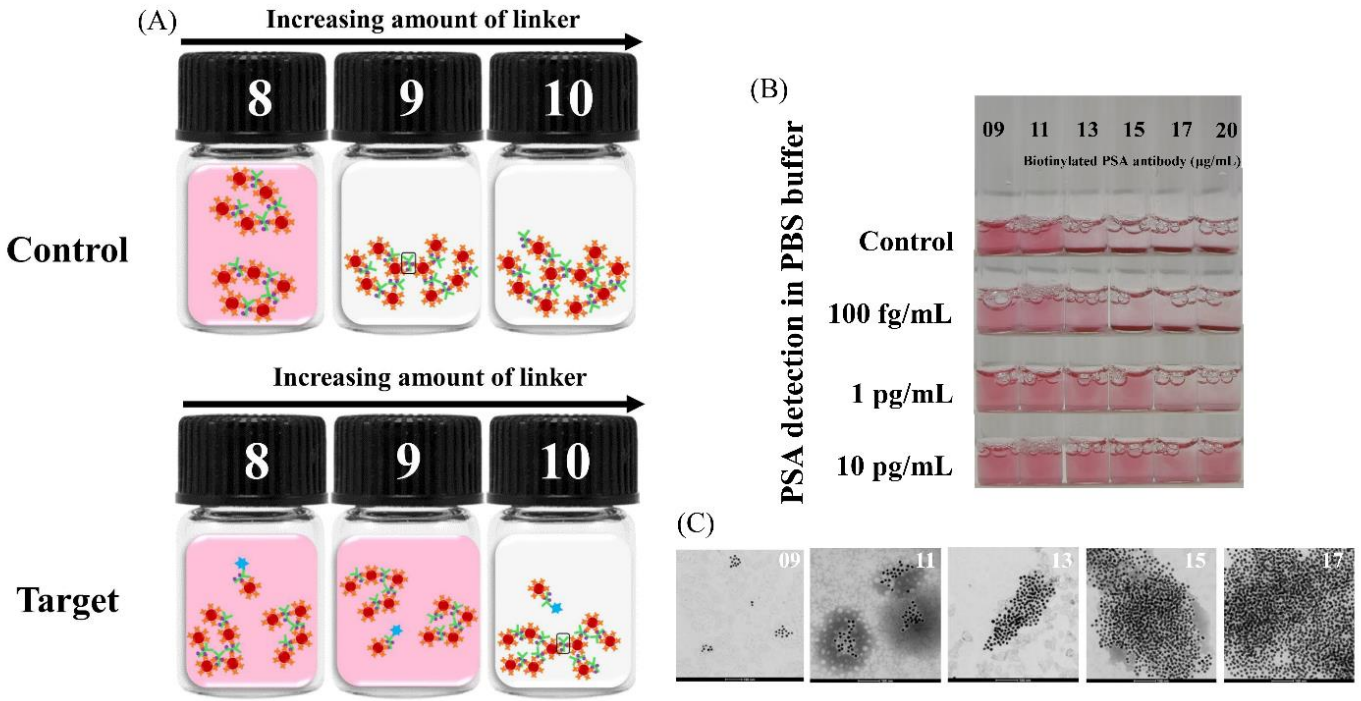

Figure III-3. (A) Scheme of BL-based immunoassay for the visible detection of PSA using b-Ab as the BL to control the extent of aggregation of st-Au NPs. SLs in the black box can connect small-scale aggregates of Au NPs to induce large-scale aggregates. Numbers on the vial lids represent the number of BLs. (B) REVC (low end region) shifts to the right while performing the BL-based assay for detecting PSA (0, 100 fg/mL, 1 pg/mL, 10 pg/mL) in PBS buffer. (C) TEM image of aggregates size at various linker concentrations (9, 11, 13, 15, and 17 μg/mL) of control in Figure III-3B.

III-3.3. Ultra-sensitive performance of the immunoassay

Based on the results of the above studies, next, I conducted an experiment to determine whether an BL-based immunoassay is capable of detecting PSA. In this experiment, I used a biotinylated anti-PSA antibody as a BL. First, I investigated the span of the REVC in PBS buffer to identify the BL concentration range in which large-scale aggregates of st-Au NPs form. As shown in Figure III-S1, the REVC span (low end) of the control is in the linker concentration range of 10–35 μg/mL, and as the PSA concentration increased from 1 pg/mL to 1 μg/mL, the REVC at each PSA concentration shifted towards a higher linker concentration. To lower the detection limit, I limited the linker concentration range to 10–20 μg/mL, which is the concentration of the REVC shift between the control and 1 pg/mL of PSA (Figure III-S1). The results confirm the REVC shift even at a concentration of 100 fg/mL of PSA (Figure III-3B). The BL-based assay has excellent sensitivity and the advantages of colorimetric methods. The reason the BL-based assay has high sensitivity is due to the way in which the Au NPs aggregate. In the conventional LSPR-based method that uses the aggregation of Au NPs, when the Au NPs aggregate to change the color of the solution, a single Au NP binds to many target species, which results in low sensitivity. However, because the Au NP aggregation and target recognition processes are independent in the BL-based assay, it achieves high sensitivity despite its reliance on color change via the aggregation of Au NPs. As shown in Figure III-3A, the affinity of streptavidin and biotin plays an important role in the Au NP aggregation process

(binding of st-Au NP and b-Ab as an BL), and the target recognition process (binding of PSA and b-Ab) involved in the antibody–antigen interaction. This independent process could help explain why the BL-based assay has a high sensitivity, as shown in Figure III-3A. As the specific linker (in the black box) is added at the boundary, particularly at the low end of the REVC in the control (linker concentrations 8 and 9), small-scale aggregates (which do not settle at a specific time) can connect with each other to form large-scale aggregates (which do settle at a specific time) and thereby exhibit a color change. As such, even if a very low target concentration is introduced into the system (to simplify the mechanism, Figure III-3A shows a solution with one target molecule), an REVC shift can be induced because the concentration at which a particular linker is present can vary. I indirectly confirmed this finding in the transmission electron microscopy (TEM) image shown in Figure III-3C (TEM images of aggregates at each concentration of the control shown in Figure III-3B: 9 μg/mL, 11 μg/mL, 13 μg/mL, 15 μg/mL, and 17 μg/mL) In the figure, I can see that as the concentration of the linker increases, the size of the aggregate gradually increases. Therefore, I see the formation of aggregates of a certain size (aggregates above a concentration of 13 μg/mL), which results in a color change. In addition, these results provide a basis for explaining that “switch-off” may occur even with a very large quantitative difference between the linker and target in the system. As shown in Figure III-3, at 1 pg/mL of the PSA concentration, the REVC occurred at a linker concentration of 17 μg/mL. The target and linker used in this experiment comprised

about 1.06×10^6 and 2.01×10^{11} molecules, respectively. As in previous research, here, I found switch-off to be possible despite the fact that the target had fewer molecules than the linker by a factor of about 2×10^5, but the exact mechanism cannot yet be explained. Figure III-3A may provide a clue regarding this mechanism, but more research is needed.

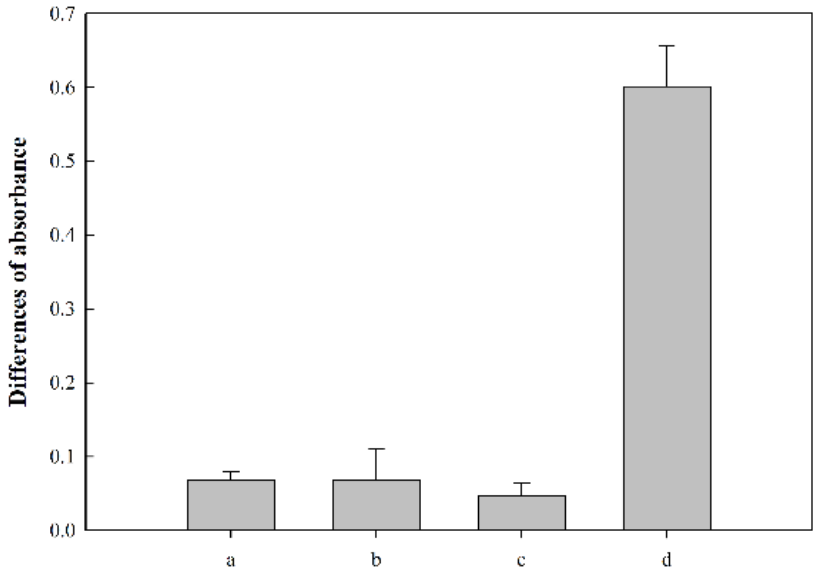

Figure III-4. Selectivity of the BL-based assay for the detection of 4 model proteins: (a) Ovalbumin, (b) streptavidin, (c) HSA, (d) PSA. The concentrations of proteins were all 10 ng/mL. The error bars are the standard deviations of 3 repeat measurements.

III-3.4. Selectivity of the BL-based immunoassay

The detection specificity of the biosensor is a crucial factor for the in-situ analysis of analytes without using any separation process. To confirm the specificity of the BL-based assay, I investigated the response of the sensor for 10 ng/mL of PSA, streptavidin, ovalbumin, and HSA (Figure III-4). The experimental results clearly showed that the difference in the absorbance of the PSA is much higher than those of the other proteins. The PSA showed an approximate 0.6 difference in the absorbance intensity, at which point I could distinguish the color change with the naked eye. However, the other proteins exhibited no statistical difference in signal intensity. These results indicate the non-specific interaction of streptavidin, HSA, and ovalbumin with b-Ab, and the negligible influences of these external proteins on PSA detection.

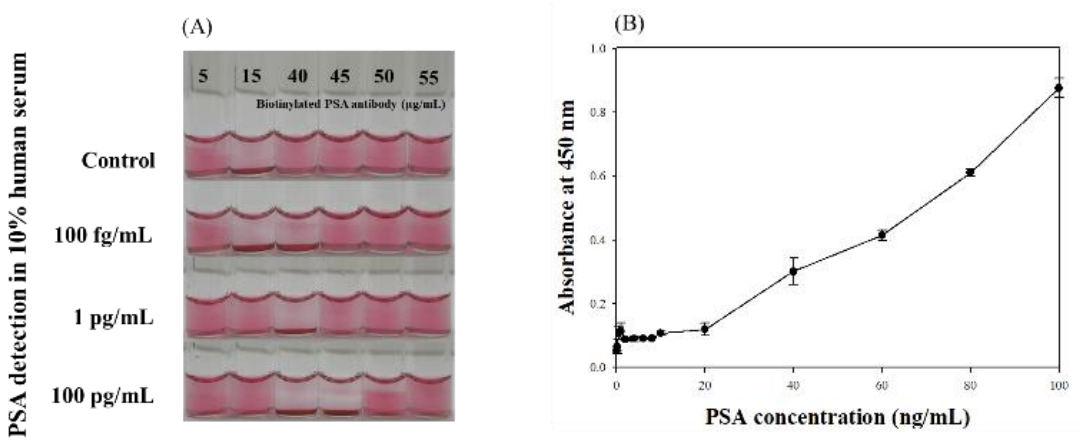

Figure III-5. (A) REVC shifts to the right while performing the BL-based assay for detection of PSA (100 fg/mL, 1 pg/mL, and 100 pg/mL) in 10% human serum. (B) The results of PSA detection in human serum by direct ELISA (from 0.2 ng/mL to 100 ng/mL).

III-3.5. Detection of PSA in serum

Next, I evaluated whether the BL-based assay was capable of detecting PSA in a real matrix. To do so more clearly, I investigated the entire concentration span of REVC (from the low to high end). As shown in Figure III-S2, I investigated the REVC in PBS, human serum, and 10% human serum in various concentrations of the b-PSA antibody (5 μg/mL, 10 μg/mL, 15 μg/mL, 20 μg/mL, 25 μg/mL, and 30 μg/mL). I observed REVCs after 15 μg/mL in the PBS buffer and 10% serum, but in the human serum, I observed the REVC from 20 μg/mL. Based on these results, I validated the BL-based assay on 10% serum, and obtained results similar to those in the PBS buffer case. As shown in Figure III-5, I detected PSA in 10% serum using the BL-based immunoassay; and in the 100-fg/mL concentrations of PSA and negative control, I could recognize the color difference at a linker concentrations ranging from 15 μg/mL to 40 μg/mL.

Table III-1. Comparison of analytical performances of different colorimetric biosensors used for PSA detection

Sensor preparation method	Biosenser principle	Detection limit	Ref.
PSA substrate–magnetic nano-carrier complexes	Magnetic nanoparticle-based biosensors	10 ng/mL	[40]
Anti-human PSA/catalase-Labelled Au NP	Reverse colorimetric immunoassay (RCIA)	0.03 ng/mL	[17]
Enzyme-cascade-amplification strategy (ECAS-CIA)	Enzyme labed immunoassay	0.05 ng/mL	[9]
Iron oxide-to-prussian blue (PB) nanoparticle (NP) conversion strategy	Colorimetric immunoassay	1.0 ng/mL	[41]
Homogenous growth of gold nanocrystals	Colorimetric immunoassay	1.0 pg/mL	[42]
Enzyme-chromogenic substrate	Colorimetric immunoassay	0.5 pg/mL	[43]
Gold nanoparticle (Au NP)−mediated copper deposition	Sandwich immunoassay	0.27 pg/mL	[44]
Anti-human PSA antibody labelled biotin	Direct ELISA	22.83 ng/mL	In this study
Gold nanoparticle aggregation with biotinylated anti-PSA antibody	BL-based immunoassay	100 fg/mL	In this study

III-3.6. Comparison of colorimetric biosensors and ELISA method

I compared detection of spiked PSA in human serum by ELISA, the most widely used colorimetric method for detection of protein biomarkers, with the BL-based assay. ELISA was performed at various PSA concentrations. As shown in Figures III-5A and III-5B, the lowest detectable concentration in the BL-based assay was 100 fg/mL. By contrast, ELISA could only detect concentrations as low as 22.83 ng/mL. Table III-1 shows different types of colorimetric biosensors for PSA detection and their detection limits. These colorimetric detection methods used various signal amplification strategies to increase sensitivity. The BL-based immunoassay used in this study also has very high sensitivity.

III-3.7. Sensitivity difference with respect to the BL design

In the suitability test for using PSA as the protein target, the BL-based assay allowed PSA detection down to 100 fg/mL concentrations. To compare the detection limits with other protein targets, I conducted a streptavidin detection experiment, in which I used biotinylated BSA as a bi-functional linker. As shown in Figure III-S3, the BL-based assay could identify streptavidin concentrations of 200 ag/200 μL. Interestingly, however, the sensitivities of the system to streptavidin and PSA were significantly different. I hypothesize the following reasons for these differences: It may be that the sensitivity difference between b-BSA and b-Ab is due to physical differences such as size and shape. As shown in Figure III-S4, b-Ab is designed such that the site binding

to the target, i.e., the antigen recognition site, is fixed, whereas b-BSA is designed such that the target can bind to biotin existing throughout BSA. Thus, when the connection to the target is switched off, b-BSA would be less affected by steric hindrance than b-Ab, so cross-linking between b-BSA and st-Au NPs would be easier. In other words, depending on how the BL is designed, the bonding forces of st-Au NPs could differ, which might change the sensitivity of the detection system. For a more accurate judgment, further studies on the effect of the reactivity of Au NPs and BLs are needed.

Previous studies have suggested various situations in which an BL was switched off and research on polyclonal antibodies has revealed that a combination of various epitopes with an BL can result in a switched-off situation by target/BL aggregates. [33] In this study, I examined whether a switch-off state could occur when a monoclonal antibody forms a PSA/b-Ab complex, and I have confirmed that biotinylated monoclonal antibodies can act as BLs. This result was expected for the following reasons. Biotin would be restricted in its affinity to bind with streptavidin by the steric hindrance effect of the PSA/b-Ab complex. In addition, when BL participates in the formation of large-scale aggregates, one BL has to cross-link with many st-Au NPs. As the cross-linking progresses, the binding force of the remaining biotin will decrease. Therefore, b-Ab that is bound to PSA is expected to have a reduced ability to form large-scale aggregates.

III-4. References

1. M. A. Ali, I. Rehman, A. Iqbal, S. Din, A. Q. Rao, A. Latif, T. R. Samiullah, S. Azam and T. Husnain, *Adv life sci*, 2014, 1, 129-138.
2. B. Madhavan, S. Yue, U. Galli, S. Rana, W. Gross, M. Müller, N. A. Giese, H. Kalthoff, T. Becker and M. W. Büchler, *International journal of cancer*, 2015, 136, 2616-2627.
3. J.-F. Masson, *ACS sensors*, 2017, 2, 16-30.
4. S. B. Nimse, M. D. Sonawane, K.-S. Song and T. Kim, *Analyst*, 2016, 141, 740-755.
5. Y. Wang, J. Dostalek and W. Knoll, *Analytical chemistry*, 2011, 83, 6202-6207.
6. G. E. N. Pauli, A. de la Escosura-Muñiz, C. Parolo, I. H. Bechtold and A. Merkoçi, *Lab on a Chip*, 2015, 15, 399-405.
7. H. Akhavan-Tafti, D. G. Binger, J. J. Blackwood, Y. Chen, R. S. Creager, R. de Silva, R. A. Eickholt, J. E. Gaibor, R. S. Handley and K. P. Kapsner, *Journal of the American Chemical Society*, 2013, 135, 4191-4194.
8. Y. Fang, Y. Li, M. Zhang, B. Cui, Q. Hu and L. Wang, *Analyst*, 2019, 144, 2186-2194.
9. Z. Gao, L. Hou, M. Xu and D. Tang, *Scientific reports*, 2014, 4, 3966.
10. D. Geißler, S. Stufler, H.-G. Löhmannsröben and N. Hildebrandt, *Journal of the American Chemical Society*, 2012, 135, 1102-1109.
11. Y. Huang, X. Liu, H. Huang, J. Qin, L. Zhang, S. Zhao, Z.-F. Chen and H. Liang, *Analytical chemistry*, 2015, 87, 8107-8114.
12. S. Krishnan, V. Mani, D. Wasalathanthri, C. V. Kumar and J. F. Rusling, *Angewandte Chemie International Edition*, 2011, 50, 1175-1178.
13. B. S. Munge, A. L. Coffey, J. M. Doucette, B. K. Somba, R. Malhotra, V. Patel, J. S. Gutkind and J. F. Rusling, *Angewandte Chemie International Edition*, 2011, 50, 7915-7918.
14. R. De La Rica and M. M. Stevens, *Nature nanotechnology*, 2012, 7, 821.
15. J. Li, H.-E. Fu, L.-J. Wu, A.-X. Zheng, G.-N. Chen and H.-H. Yang, *Analytical chemistry*, 2012, 84, 5309-5315.
16. L. Xiao, A. Zhu, Q. Xu, Y. Chen, J. Xu and J. Weng, *ACS applied materials & interfaces*, 2017, 9, 6931-6940.
17. Z. Gao, M. Xu, L. Hou, G. Chen and D. Tang, *Analytical chemistry*, 2013, 85, 6945-6952.
18. N. Malashikhina, G. Garai-Ibabe and V. Pavlov, *Analytical chemistry*, 2013, 85, 6866-6870.
19. Y. Hu, L. Li and L. Guo, *Sensors and Actuators B: chemical*, 2015, 209, 846-852.
20. Y. Liu, L. Zhang, W. Wei, H. Zhao, Z. Zhou, Y. Zhang and S. Liu, *Analyst*, 2015, 140, 3989-3995.

21. J. Xu, M. Shi, W. Chen, Y. Huang, L. Fang, L. Yao, S. Zhao, Z.-F. Chen and H. Liang, *Chemical Communications*, 2018, 54, 2719-2722.
22. C.-H. Chao, C.-S. Wu, C.-C. Huang, J.-C. Liang, H.-T. Wang, P.-T. Tang, L.-Y. Lin and F.-H. Ko, *Microelectronic Engineering*, 2012, 97, 294-296.
23. C. d. L. de Morais, J. C. Carvalho, C. Sant'Anna, M. Eugênio, L. H. Gasparotto and K. M. Lima, *Analytical Methods*, 2015, 7, 7917-7922.
24. J. Kang, Y. Zhang, X. Li, L. Miao and A. Wu, *ACS applied materials & interfaces*, 2015, 8, 1-5.
25. Y. Zhang, I. D. McKelvie, R. W. Cattrall and S. D. Kolev, *Talanta*, 2016, 152, 410-422.
26. R. J. Babaian, D. A. Johnston, W. Naccarato, A. Ayala, V. A. Bhadkamkar and H. A. Fritsche, *The Journal of urology*, 2001, 165, 757-760.
27. R. A. Bok and E. J. Small, *Nature Reviews Cancer*, 2002, 2, 918.
28. F. Mannello and G. Gazzanelli, *Breast Cancer Research*, 2001, 3, 238.
29. F. C. Mashkoor, J. N. Al-Asadi and L. M. Al-Naama, *Cancer epidemiology*, 2013, 37, 613-618.
30. J.-M. Nam, C. S. Thaxton and C. A. Mirkin, *science*, 2003, 301, 1884-1886.
31. C. S. Thaxton, R. Elghanian, A. D. Thomas, S. I. Stoeva, J.-S. Lee, N. D. Smith, A. J. Schaeffer, H. Klocker, W. Horninger and G. Bartsch, *Proceedings of the National Academy of Sciences*, 2009, 106, 18437-18442.
32. J. Hahn, E. Kim, Y. S. You, S. Gunasekaran, S. Lim and Y. J. Choi, *Journal of food science*, 2017, 82, 2321-2328.
33. S. Lim, O. K. Koo, Y. S. You, Y. E. Lee, M.-S. Kim, P.-S. Chang, D. H. Kang, J.-H. Yu, Y. J. Choi and S. Gunasekaran, *Scientific reports*, 2012, 2, 456.
34. Y. You, S. Lim, J. Hahn, Y. J. Choi and S. Gunasekaran, *Biosensors and Bioelectronics*, 2018, 100, 389-395.
35. E. Hauser and J. Lynn, *Industrial & Engineering Chemistry*, 1940, 32, 659-662.
36. G. Kc, *Anal. chem*, 1995, 67, 735-743.
37. G. Presnova, M. Y. Rubtsova, D. Presnov, V. Grigorenko, I. Yaminsky and A. Egorov, *Biochemistry (Moscow) Supplement Series B: Biomedical Chemistry*, 2014, 8, 164-167.
38. J. Anker and W. Hall, *Nature Materials*, 2008, 7, 442.
39. L. Chaiet and F. J. Wolf, *Archives of biochemistry and biophysics*, 1964, 106, 1-5.
40. K. Stubenrauch, U. Wessels, U. Essig, F. Kowalewsky, R. Vogel and J. Heinrich, *Journal of pharmaceutical and biomedical analysis*, 2013, 72, 208-215.
41. W. Haiss, N. T. Thanh, J. Aveyard and D. G. Fernig, *Analytical chemistry*, 2007, 79, 4215-4221.
42. G. A. Suaifan, C. Esseghaier, A. Ng and M. Zourob, *Analyst*, 2013, 138, 3735-3739.

43. G. Fu, S. T. Sanjay and X. Li, *Analyst*, 2016, 141, 3883-3889.
44. C. Cao, X. Li, J. Lee and S. J. Sim, *Biosensors and Bioelectronics*, 2009, 24, 1292-1297.
45. W. Lai, D. Tang, J. Zhuang, G. Chen and H. Yang, *Analytical chemistry*, 2014, 86, 5061-5068.
46. Y. Liu, Z. Zhang, J. Yu, J. Xie and C. M. Li, *Analytica chimica acta*, 2017, 963, 129-135.

III-5. Appendix: Optimization of BL-based assay for detection of protein targets

III-5-1. Optimization of degree of REVC shift

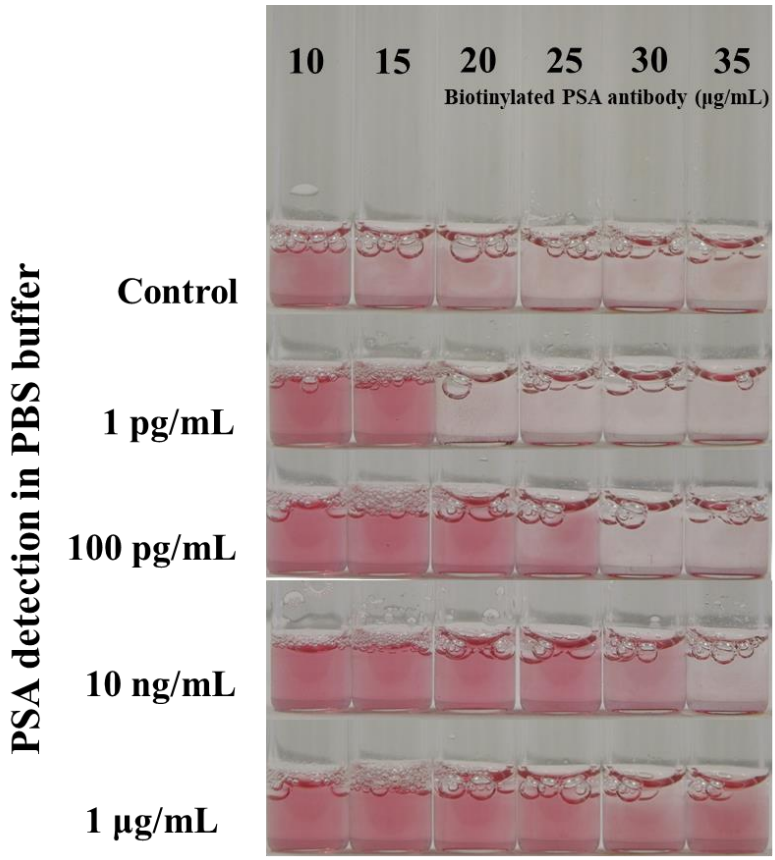

Figure III-S1. REVC shifts to higher linker concentrations with the increase in PSA concentrations (from 1 pg/mL to 1 µg/mL) by 100-fold to confirm the broad detection range of the SL-based immunoassay in PBS buffer.

III-5-2. Optimization of shift in REVC differences

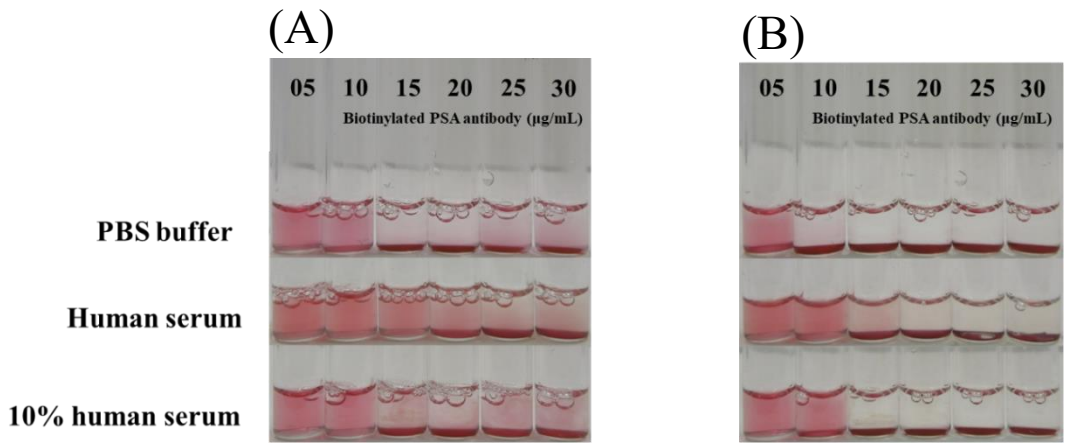

Figure III-S2. The REVC difference in 3 control samples (PBS buffer, Human serum, and 10% human serum) after (A) 2 h and (B) overnight.

III-5-3. Shift in REVC of the BL-based assay for detecting streptavidin

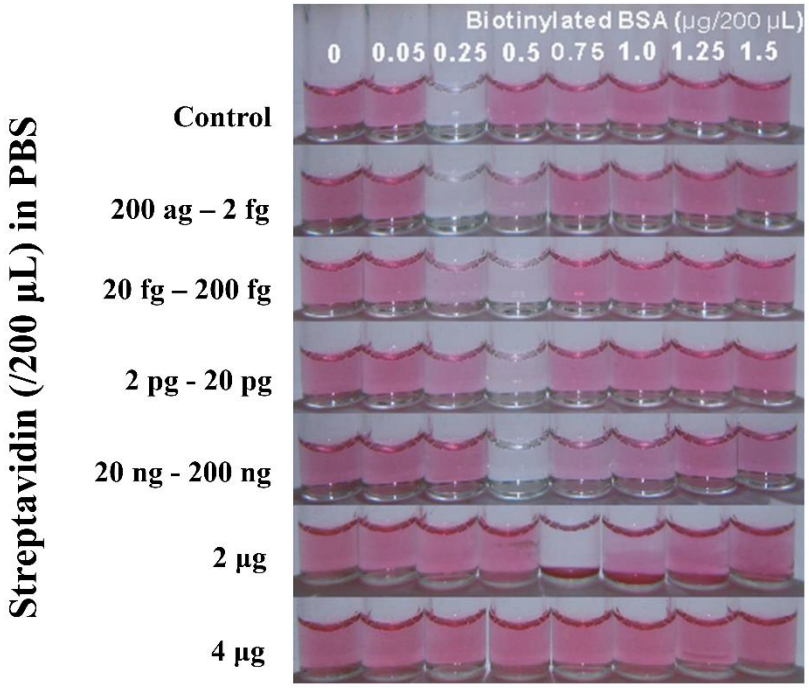

Figure III-S3. Shift in REVC after 3 h of the BL-based assay for detecting streptavidin (from 200 ag/200 µL to 4 µg/200 µL) in PBS buffer using a fixed concentration of st-Au NPs (absorption :0.21 at 531.5 nm for 1/10 dilution sample).

III-5-4. Schematic representation of the switching off process

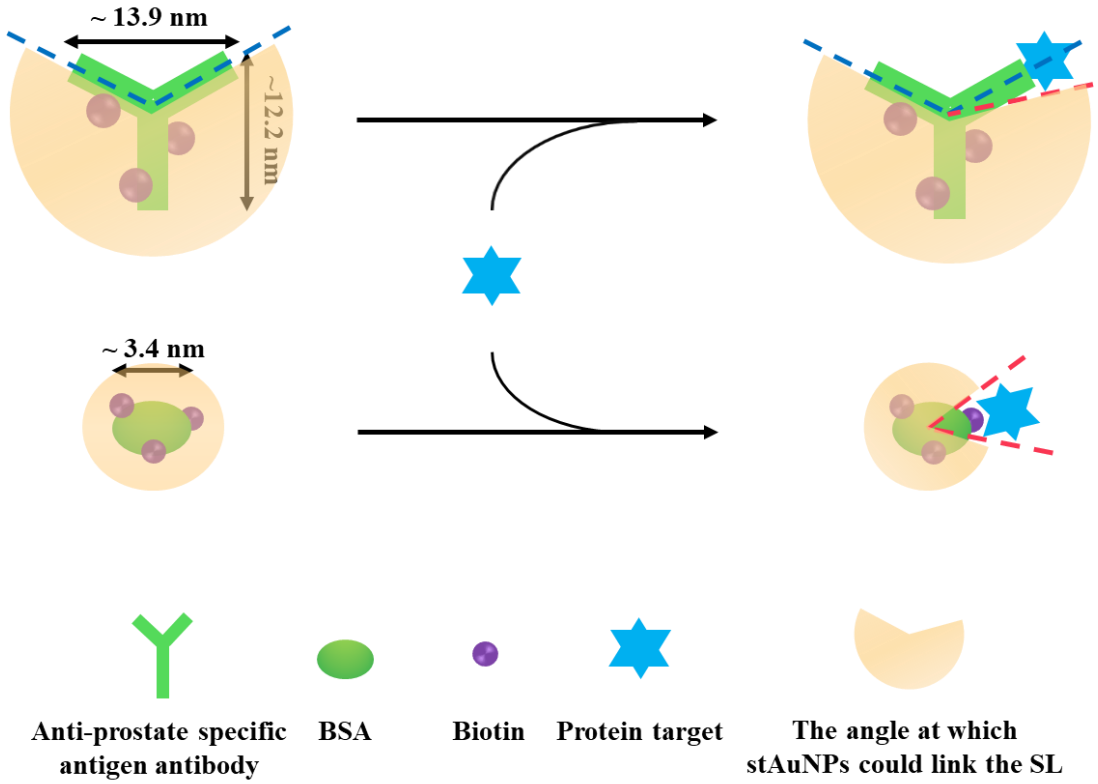

Figure III-S4. Schematic representation of the physical difference between the switching off process in b-Ab and b-BSA. B-Ab has a determined target recognition site, whereas b-BSA has a target recognition site determined at random. Therefore, b-BSA is less affected by steric hindrance than b-Ab when bound to the st-Au NPs in the switching-off situation.

Chapter IV. Development of a portable lab-on-a-valve device for making primary diagnoses based on gold-nanoparticle aggregation induced by bi-functional linker

IV-1. Introduction

Novel bioengineering and diagnostic technologies for the detection of pathogens are expanding their application to a variety of fields, including molecular diagnostics, food-safety testing, medical diagnostics, and environmental monitoring. [1-4] The development of such platforms that enable miniaturization, rapid diagnosis, and reduced cost for on-site diagnoses represents an important advance. [5-7] To date, standard testing for pathogen detection has been based on traditional cell-culture methods that require at least 48 hours. [8] In addition, the enzyme-linked immunosorbent assay (ELISA) is widely used to detect pathogens with high sensitivity and selectivity. [9, 10] However, these methods are difficult to apply in the field because of their need for complex, labour-intensive processing steps and well-trained operators. [11] Therefore, it is essential to develop a diagnostic method that enables quick and inexpensive testing without the need for peripheral devices. Device miniaturization techniques improve portability and minimize the need for bulky laboratory infrastructures in primary-diagnosis settings. [12, 13] In addition, the development of these compact diagnostic devices widens the range of strategies for disease monitoring and management. [14]

Recently, lab-on-a-valve (LOV) devices have emerged as a new technology for flow control. [15-17] LOV devices have the advantage of being directly manipulated by a programmable flow-based platform that can adopt different coupling modes and

controlled fluid movement, as compared to the lab-on-a-chip. [18] Flow analyses by LOV devices seem to be suitable for the development of portable analysis systems in that this technology reduces instrument size and reagent and energy consumption, which are important benefits for field systems, while simplifying the work required for analysis. [19]

In this study, I applied flow analysis to bi-functional linker (BL)-based analysis using 3-way valve chambers (3-VCs). The 3-way valve, which provides a convenient and economical means of selecting various flow rates and directions, plays a crucial role in almost all industrial processes, including the food field. [20-22] In addition, the 3-way valve can control the flow of fluid via a simple operation and can be applied to various fluids based on their materials, volume, and ranges of temperature and pressure. [23, 24] However, a 3-way valve that is sealable, portable, and easy to operate has not yet been developed for use as a reaction chamber for bioassays. In addition, both disposable syringes and syringe filters, which have the advantages of sterilization, low cost, and wide application, can comprise a good biosensing application kit in the field. [25-28]

Colorimetric detection based on gold-nanoparticle aggregation has attracted interest as a novel alternative for on-site detection due to its simplicity and the fact that it needs no sophisticated equipment or technology. [29-32] The gold-nanoparticle aggregation-based colorimetric method has a limitation in that its detection signal is weak when detecting a relatively large target such as a pathogen because the spectral

aggregation shift decreases as the distance between Au NPs increases. [33] Therefore, in our previous research, our research group proposed the use of a bi-functional linker to induce the large-scale aggregation of Au NPs and to enhance the detection signal by sedimentation of the aggregates. This new colorimetric detection method is expected to increase the capability of on-site detection.

In this study, I first developed a portable kit comprising a 3-way valve for the on-site detection of *Salmonella* Typhimurium. This kit is based on the use of colorimetric detection by the precipitation of gold nano-aggregates (Au NAs) and a novel bi-functional linker to amplify the visible signal by the aggregation of Au NPs. [34-37] In addition, for quick on-site detection, I introduced filtration into the device as a strategy for improving the visual detection signal.

IV-2. Materials and Methods

IV-2-1. Chemicals, reagents, and instruments

I purchased streptavidin, phosphate-buffered saline (PBS), 1-mM tetrachloroaurate, and bovine serum albumin (BSA) from Sigma-Aldrich (Madison, WI), and tetraborate pH standard solution from Wako Pure Chemicals (Osaka, Japan). I purchased anti-*Salmonella* polyclonal antibody (biotin) from Abcam (Cambridge, MA) and vials, ethanol, and trisodium citrate from local suppliers.

As the buffer in the synthesis of 13-nm Au NPs, I used sterilized distilled water, which I prepared with 1% (w/v) tri-sodium citrate as a reducing agent. The buffers used for the BL-based assay for the detection of streptavidin as a model target and *Salmonella* were 0.01 mol/L PBS (pH 7.4) prepared with 0.1% and 0.5% (w/v) BSA, respectively, for blocking, and 0.01 mol/L tetraborate pH standard solution (pH 7.4) for diluting the streptavidin.

I performed the BL-based immunoassay in 3-VCs purchased from a local supplier, and filtered the Au NAs using a 50-mL syringe (local supplier) and syringe filters (Hyundai Micro, South Korea). To determine the assay absorbance, I used a UV-1700 spectrophotometer (Shimadzu, Japan). The size (number) of the Au NAs was determined using a Zetasizer (Nano ZS, Malvern Instruments Ltd., Worcestershire, UK).

IV-2-2. Preparation of colloidal streptavidin-coated Au NPs

I prepared colloidal Au NPs with an average size of 13 nm by reducing tetra-chloroaurate with tri-sodium citrate, which is a well-established citrate reduction method.[38] I verified the particle size by transmission electron microscopy (TEM, JEM1010, JEOL, Japan) and UV-Vis spectroscopy (UV-1700 PC, Shimadzu). The synthesized Au NPs had an ultraviolet-visible spectrum peak (λ_{max}) at 520±1.0 nm. Based on the absorbance value (0.4 in a 1/10 dilution sample), the concentration of the Au NPs was estimated to be ~7×10^{12} particles/mL. The prepared Au NPs were coated with streptavidin for surface functionalization using an electrostatic adsorption procedure.[39] To functionalize the prepared Au NPs, I coated 40 μg of streptavidin dissolved in a tetra-borate solution (pH 7.4) onto 600 μL of the citrate-stabilized Au NPs with an absorbance of 0.4 (1/10 dilution sample) at 520±1.0 nm. To remove unbound streptavidin, centrifugation was conducted at 10,000 *g* for 30 min. Then, the supernatant containing the unbound streptavidin was removed and washed off and then mixed with 0.5% (w/v) BSA dissolved in PBS as a blocking buffer. The Au NPs coated with streptavidin molecules (st-Au NPs) exhibited a peak at 531.5 ± 0.5 nm at a concentration with a peak absorbance value of 0.4 (1/10 dilution sample4 in their UV-Vis spectra.

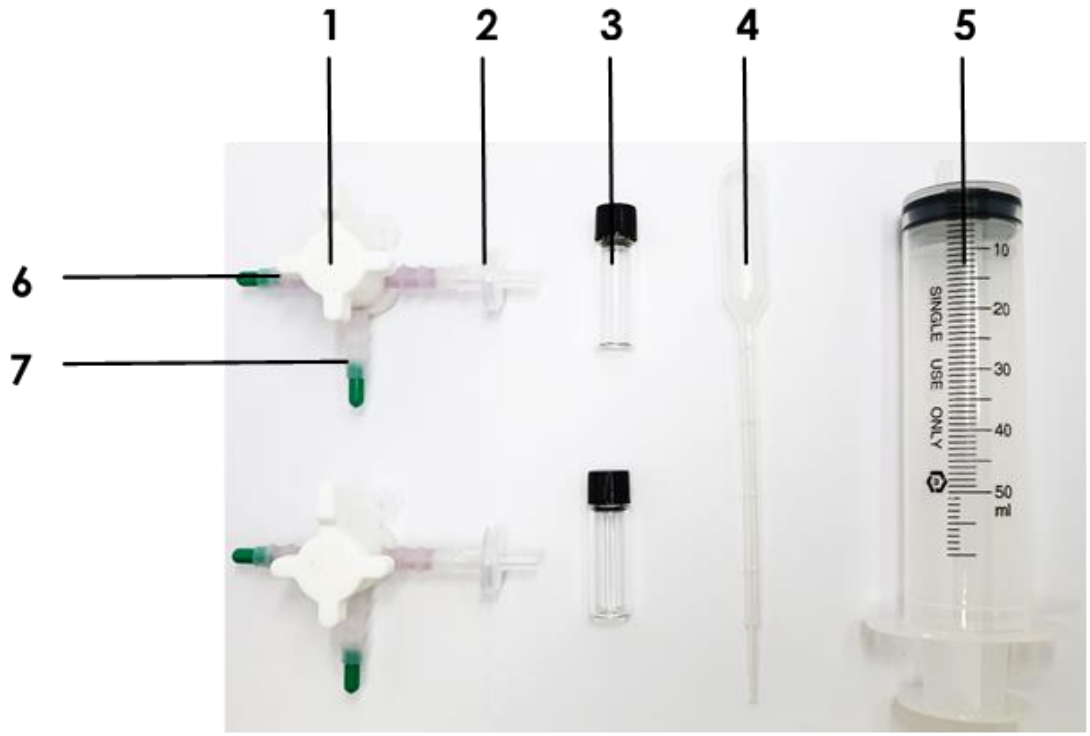

Figure IV-1. Photograph of the portable detection kit, which consists of the following materials and reagents: (1) 3-way valve that serves as a storage and reaction chamber, (2) a syringe filter (0.45 μm, PVDF, hydrophilic), (3) a signal-indication vial, (5) a disposable pipette used to inject the test sample, (5) a 50-mL syringe for applying pressure to the filter, (6) the reaction chamber containing the linker (b-Ab) solution, and (7) the storage chamber containing the st-Au NP solution.

IV-2-3. Fabrication of the portable kit

The major objective in developing the prototype kit was to produce a low-cost portable reaction chamber with a 3-way valve to provide an easy-to-use device for primary diagnosis. As shown in Figure IV-1, the portable kit consists of a 3-way valve that acts as a reaction chamber, a 50-mL syringe that is used for sample injection and as a filter press, and a syringe filter that filters out Au NAs to obtain a rapid detection signal. To store 200 μL of streptavidin-coated Au NPs (st-Au NPs) and handle the total volume of 400 μL in the reaction, I determined the required pipe length and diameter of the 3-VC to be 16 mm and 4 mm, respectively. To minimize interaction of the device material with proteins, I selected polyvinylidene fluoride (PVDF, hydrophilic) as the 3-VC material.

Table IV-1. Comparision of the material, pore size, and filtering ability of the syringe filters

Types	Pore size (μm)	Filtering (PBS)	Filtering (milk)	Filtering (0.1% milk)
Mixed Cellulose Ester (MCE)	0.2	Possible	-	-
Mixed Cellulose Ester (MCE)	0.45	Possible	Less	Less
Polyethersulfone (PES)	0.2	Possible	-	-
Polyethersulfone (PES)	0.45	Possible	Less	Less
Cellulose Acetate (CA)	0.45	Possible	Less	Less
Polyvinylidene Fluoride (PVDF, hydrophilic)	0.2	Possible	-	Less
Polyvinylidene Fluoride (PVDF, hydrophilic)	0.45	Possible	Possible	Possible
Polyvinylidene Fluoride (PVDF-D, hydrophobic)	0.2	Possible	-	Less
Polyamide (NYLON)	0.2	Possible	-	Less
Polyamide (NYLON)	0.45	Possible	Less	Possible
Polytetrafluoethylene (PTFE-D)	0.2	Possible	-	-
Polytetrafluoethylene (PTFE-D)	0.45	Possible	Less	Possible
Polytetrafluoethylene (PTFE-H)	0.2	Possible	Less	Possible
Polytetrafluoethylene (PTFE-H)	0.45	Possible	-	Less

IV-2-4. Optimization of the syringe filter

In the BL-based assay, the visible detection signal is amplified by the loss of colour following the precipitation of the large scale-aggregates of Au NPs induced by the BL. In this study, since a filter was introduced to quickly obtain the detection result, experiments were conducted to compare the performances of various filters and determine which was most effective. As shown in Table IV-1, filters comprising various materials (mixed cellulose ester, polyethersulfone, cellulose acetate, polyvinylidene fluoride, polyamide, and polytetrafluoethylene) and sizes (0.2 μm and 0.45 μm) were used in the filtration of Au NAs in PBS, milk, and 0.1% milk. The total 400-μL volume of the st-Au NP solution was filtered through each syringe filter.

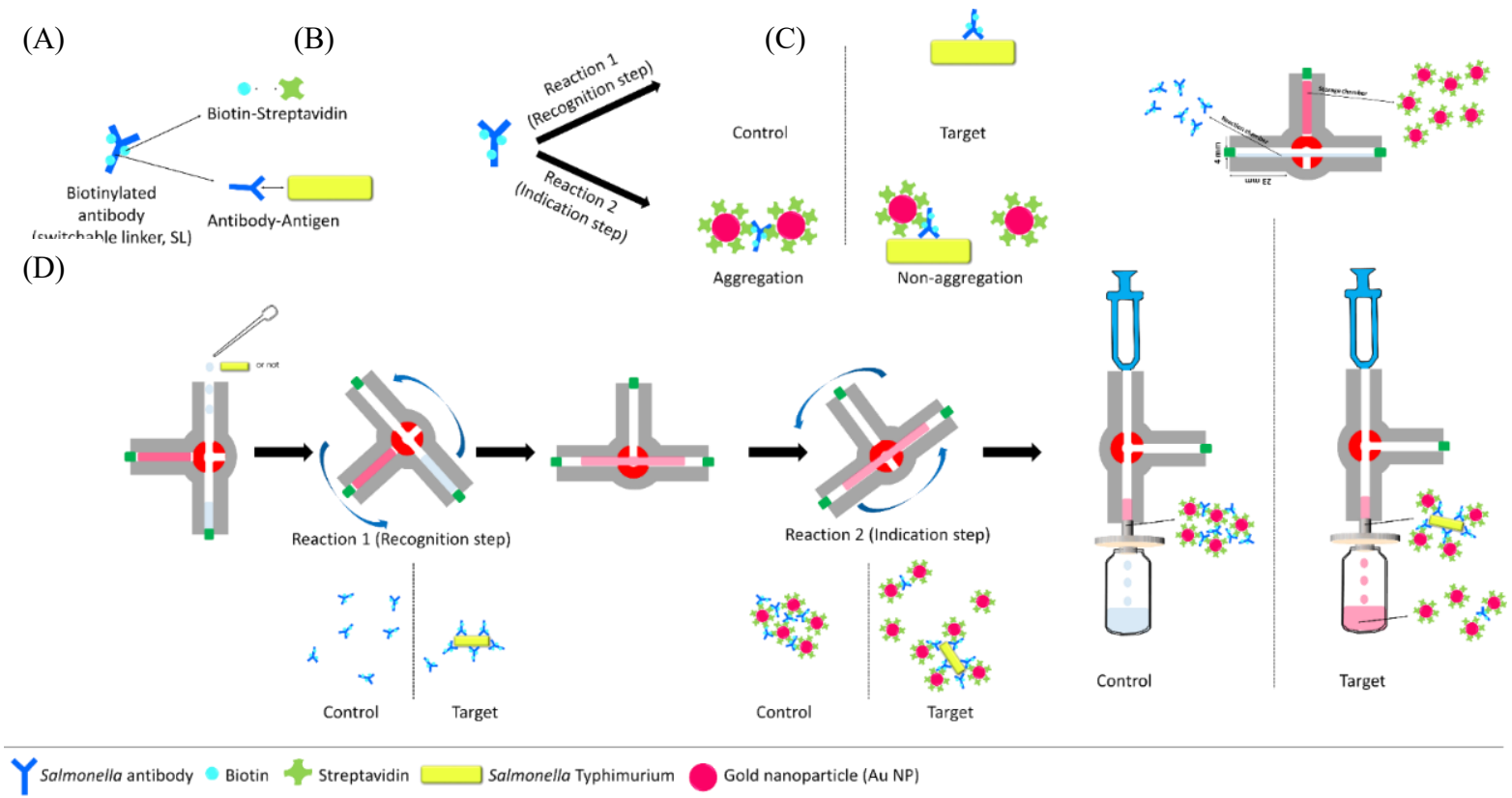

Figure IV-2. Schematic of detection principles and procedure. (A) Biotinylated *Salmonella* antibody (b-Ab) can bridge to st-Au NP (by the biotin–streptavidin interaction) and target *Salmonella* (via the antibody-antigen interaction). (B) The BL-based assay is performed in two sequential steps: The first reaction serves as a target recognition step, in which BL reacts with the target bacteria. The second reaction serves as a signal indication step, in which BL reacts with st-Au NPs. (C) The configuration of the 3-VC comprising the reaction chamber with BLs and the storage chamber with st-Au NPs. (D) The procedure of the BL-based assay in the 3-VC.

IV-2-5. Detection procedure

The BL-based assay, developed in a previous study, was performed using the portable kit. As shown in Figures IV-2C and IV-2D, BL-based assays were performed in a total reaction volume of 400 µL containing 200 µL of st-Au NP solution at a fixed concentration, 100 µL of biotinylated BSA (b-BSA) or biotinylated polyclonal *Salmonella* antibody (b-Ab) as the BL, and 100 µL of a test sample (PBS at pH 7.4)6 First, 100 µL of b-Ab or b-BSA was prepared in a closed chamber of the 3-VC and 200 µL of st-Au NPs was prepared in the closed pipe of the 3-VC. One hundred microliters of the test sample was injected into one pipe of the 3-VC using the syringe, and then this 3-VC mixture was turned and shaken several times. After an adequate reaction time, I opened the valve to allow the mixture to react with the st-Au NPs. After a sufficient reaction time, I filtered the Au NAs through the syringe filter (0.45 µm, PVDF) to obtain a visible detection signal.

Prior to performing the BL-based assays for the detection of *Salmonella* Typhimurium, I had to determine the range of the BL (b-Ab) concentration exhibiting visible colour change (REVC). An assay was performed in PBS at various b-Ab concentrations (10–45 µg/mL). Based on the REVC results, I select the concentrations of 13 to 15 µg/mL to be the most effective in clearly showing the colour change at the low end of REVC.

IV-2-6. Optimization of secondary reaction time for filtration

To filter out the Au NAs, the change in the sizes of the Au NAs over time was measured using a UV-Vis spectrometer and a Zetasizer, respectively. As BLs, 10 μm and 13 μm of biotinylated Salmonella polyclonal antibodies were used as control and aggregates samples, respectively. I added 100 μm of st-Au NP to each concentration and tracked the absorbance at the maximum peak and the sizes every minute or two using the UV-Vis spectrometer and Zetasizer, respectively.

IV-2-7. Statistical analysis

The data represent the average of at least three independent experiments or measurements.

IV-3. Results and discussion

IV-3-1. Optimization of 3-way valve chamber (3-VC)

To apply the 3-VC to the BL-based assay, it was necessary to optimize the material, the pore and bore sizes of the tubes, the maximum volume, and the loss volume. To minimize friction with the solution, among the 3-VC materials considered were diene difluoride (PVDF), polypropylene/polyethylene (PP/PE), and polyvinyl chloride. Ultimately, PVDF was selected due to its low loss volume with the system solution for every pore size. To select the final volume of the 3-way valve, using inner and outer diameters of 4 mm, 6 mm, and 8 mm and 6 mm, 8 mm, and 10 mm, respectively, I considered the compatibility of the syringes and syringe filters and their application to the assay. As they were found to be applicable to the assay under all volume conditions, I selected a valve with a 4-mm inner diameter and 6-mm outer diameter that was compatible with the syringe and syringe filter. Finally, a 3-way valve consisting of PVDF material with an inner diameter of 4 mm and an outer diameter of 6 mm was finally determined to be most suitable as a portable device for field application of the BL-based assay.

IV-3-2. The BL-based immunosensing mechanism by 3-VC

Figure IV-2 shows the proposed BL-based immunosensing mechanism for the on-site detection of *Salmonella* Typhimurium using the developed kit. The BL-based assay can induce the aggregation of st-Au NP with b-Ab and detect the target bacteria

in a real matrix. As shown in Figures IV-2A and IV-2B, I designed the BL (biotinylated antibody) to have two reactions: target recognition (the antibody–antigen immune response) and signal recognition (biotin–streptavidin binding response). Generally, the BL-based assay is performed in two sequential steps. First, the target and the BL undergo a sufficient reaction. Thereafter, depending on the presence or absence of the target, the quantitatively readjusted BLs react with st-Au NPs. When the BLs are bound to their targets, their ability to cross-link with st-Au NP is limited. I refer to this state as the linker being switched-off. Therefore, since the BL is switched off by the target, the degree of aggregation of the st-Au NPs is changed, so the BL-based assay can exhibit a visible colour-fading signal depending on the presence or absence of the target.

In this study, a 3-VC was introduced in the BL-based assay. As shown in Figure IV-2C, the 3-VC consists of a storage chamber and a reaction chamber. The storage chamber contains 200 μL of st-Au NPs solution and the reaction chamber contains 100 μL of biotinylated *Salmonella* antibody (b-Ab) solution. The amount of BL required to induce aggregation of st-Au NPs depends on the 'concentration' of the target in the system. There is also a range of BL concentrations for a given concentration of the target and st-Au NPs that leads to large-scale aggregation and a visible colour change by precipitation of the aggregates, which is known as the REVC. Therefore, the BL can be distinguished as having two regions, i.e., the REVC and the region with no aggregation of st-Au NPs and no colour change (more specifically, the

BL concentration range can actually be divided into three parts, which are not explained here) The BL-based assay can identify the target organism based on the REVC shift in response to the 'switching-off' of the BL by the target.

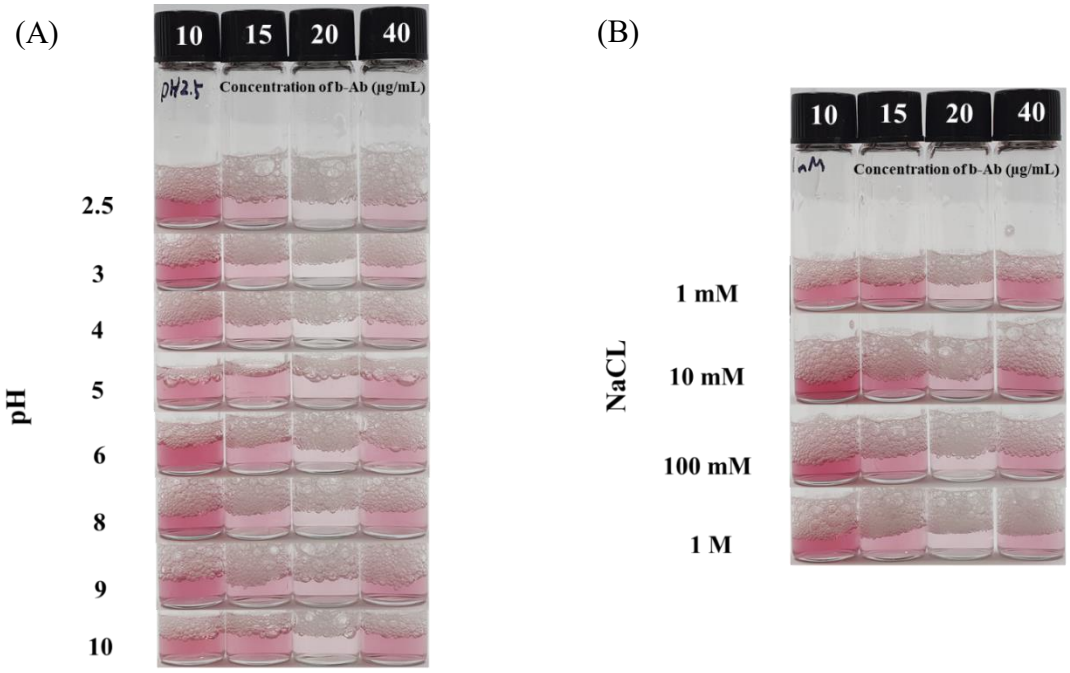

Figure IV-3. REVC shift of the control using 3-way valve chamber and syringe filter at various system conditions: (A) pH 2.5, 3, 4, 5, 6, 8, 9, 10, (B) 1, 10, 100 mM, and 1 M of NaCL.

IV-3-3. System stability of pH and salt conditions

Various and complex components in food are likely to interfere with the detection system. In particular, various pH and high salt concentrations in foods are one of the main causes of biosensor inhibition. In particular, the main factor of Au NP aggregation in this detection system is biotin-streptavidin binding force. In areas where this system will be used, there is no way to remove salt and adjust the pH of the system, so these harsh conditions have to be checked. Streptavidin is a protein as known for its high thermal and mechanical stability. Therefore, stability testing of this system was conducted with emphasis on salt and pH resistance. As shown in Figure IV-3, the system confirmed the REVC shift of the control under all pH and salt conditions. As a result, the system was stable under all conditions used in the experiment.

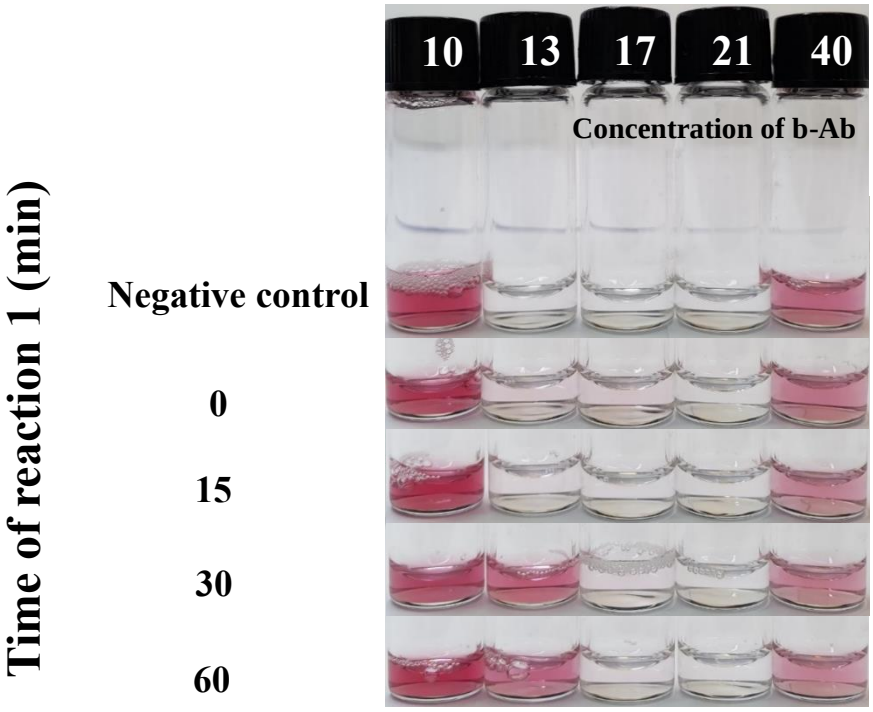

Figure IV-4. The effect of reaction time 1 with the negative control and *Salmonella* Typhimurium. Shift in REVC with increasing reaction times between b-Ab and the presence of 10^5 CFU/mL of *Salmonella* Typhimurium for 120 min after adding 100 uL of st-Au NPs (absorption: 0.4 @ 530±0.5 nm) in a 400-uL total test system volume using the 3-VC to determine the optimal time of 1st reaction. After 30 min, the REVC shifts at a linker concentration of 13 µg/mL.

IV-3-4. Determination of reaction time (first reaction time) for targets to crosslink with bi-functional linker

The BL used in this study was designed based on an antibody with biotins, and unlike the ELISA, a specific BL concentration is used in the BL-based assay without any washing step. Therefore, it is necessary to confirm the activity of the BL reacting with the target. In doing so, I tried to optimize the first reaction time of this assay, i.e., the reaction between the BL and the target in the 3-VC. As shown in Figure IV-4, 10 μg/mL of target *Salmonella* Typhimurium reacted with 10 μg/mL to 40 μg/mL of b-Ab as BLs for 0 min, 15 min, 30 min, and 60 min, and then the st-Au NPs were treated to observe the change in the REVC. After 30 minutes, an REVC shift was observed at a linker concentration of 13 μg/mL.

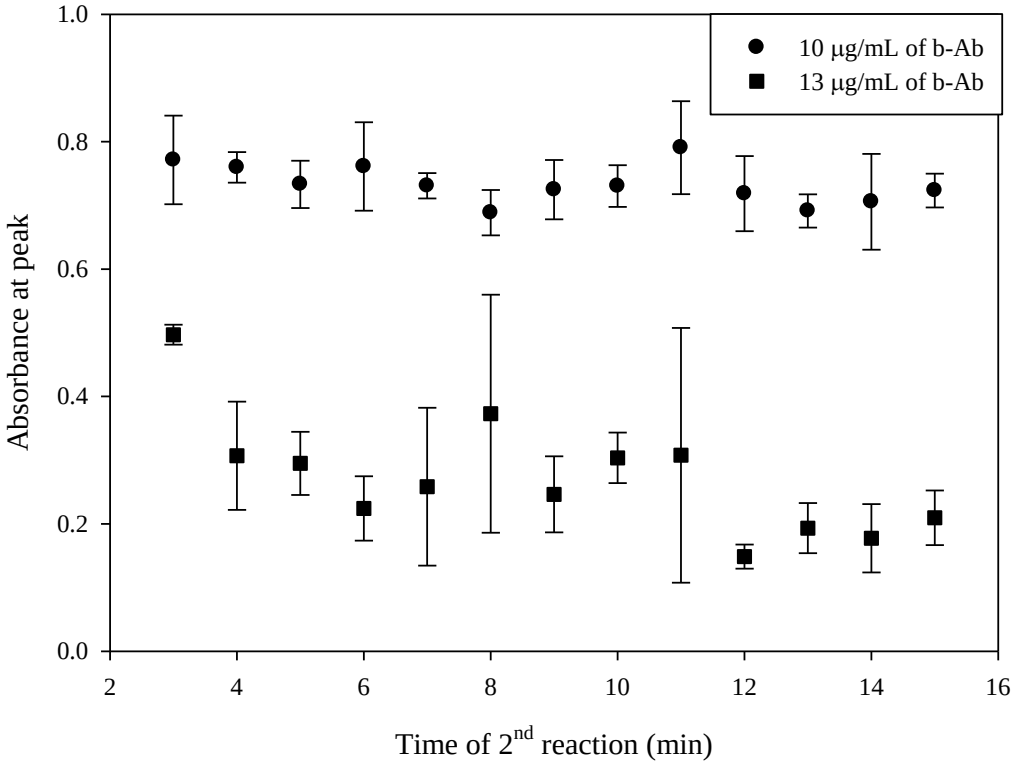

Figure IV-5. Finding the optimal time of 2nd reaction to filter the aggregates of st-Au NPs. The tracking results of size change of Au NAs over 15 minutes by UV-Vis spectrophotometer.

IV-3-5. Determination of reaction time (second reaction time) for producing the REVC signal using filter

Bi-functional linkers can play the roles of both crosslinking the Au NPs and binding the target bacteria, both of which are mutually limited. In other words, in the sequential steps of the BL-based assay, when the BL is combined with the target bacteria, it is switched off and could not play a role in inducing aggregation of Au NPs. The BL that is not bound to the target induces large-scale aggregation of Au NPs, which can eventually produce a visual signal whose color fades as it slowly precipitates out over time (up to 2 hours without shaking). The second step of this assay, which determines the REVC, consists of an aggregation reaction of the combination of streptavidin and biotin and a precipitation reaction based on the size of the Au NAs, the latter being the rate-determining step. Therefore, in this study, a filter was applied to the BL-based assay to filter out Au NAs of a certain size to minimize the time required for precipitation and thereby obtain visual signals more quickly.

To filter out Au NAs, it was necessary to track the size of the aggregates. As shown in Figure IV-5, the maximum peak of the Au NPs was tracked in 1-min increments, and the time to reach an absorbance of 0.2, which provides a clearly visible difference from the st-Au NP colloid without aggregation, was 12 min. This result represents a dramatic reduction in the reaction time compared to the conventional method, which requires a second reaction time of up to 2 h.

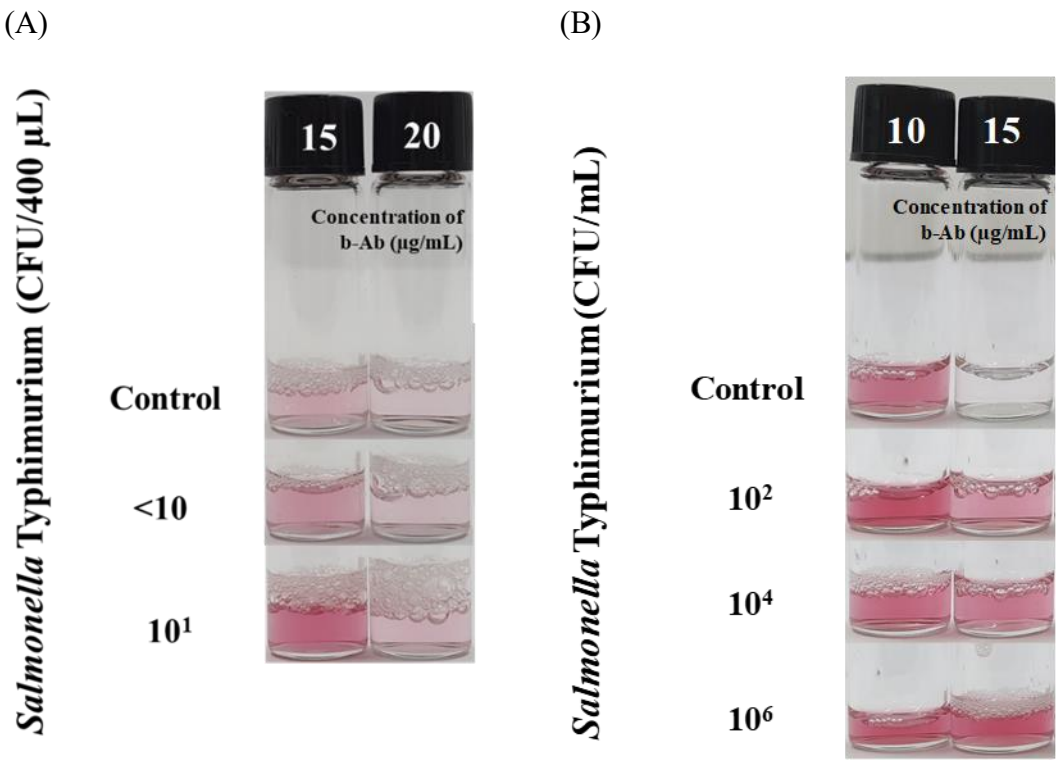

Figure IV-6. Evaluation of the BL-based immunoassay to the detection of S. Typhimurium using the developed kit. The REVC shift at low end after performing the BL-based assay for on-site detection of *S.* Typhimurium in concentrations of (A) 0, <10, 10^1 CFU/400 µL and (B) 0, 10^2, 10^4, 10^6 CFU/mL.

IV-3-6. Evaluation experiments

To evaluate the performance of the developed device, I used it to detect *Salmonella* Typhimurium on the basis of the optimized parameters at various target concentrations (10^1 CFU/mL, 10^2 CFU/mL, 10^4 CFU/mL, and 10^6 CFU/mL). As shown in Figure IV-6 (B), the REVC shift occurred at a linker concentration of 15 μg/mL, as compared to the control in all the tested *Salmonella* Typhimurium samples. In addition, as shown in Figure IV-6 (A), to identify an LOD of the BL-based assay using 3-VC and syringe filter, *Salmonella* Typhimurium with the concentrations (0, <10, 10^1 CFU/400 μL) were tested. The assay was evaluated by the naked eye after filtering of Au NAs. As a result, the clear color change (REVC) in 15 μg/mL of b-Ab was seen only in the test sample of *Salmonella* Thpymurium (10^1 CFU/400 μL). Therefore, the LOD of the BL-based assay using 3-VC was determined to be 10^1 CFU/400 μL.

Since the conventional BL-based assay is based on the precipitation of Au NAs, up to two hours is required to confirm the results. However, in the proposed device, a filter was introduced so that when the Au NAs grow to a certain size that can be filtered, the whole detection time can be reduced by shortening the time required for settling. By applying the filter, the detection result can be quickly confirmed, but I found there to be a volume difference in the filtered system depending on the pressure applied to the filter. In addition, depending on the aggregation mechanism between the target and the Au NPs for each linker concentration, there

was a difference in the color concentration because of the size of the aggregates and the number of Au NPs that did not participate in the reaction. Therefore, when using the proposed apparatus, when selecting a specific linker density, it is necessary to select a section in which the difference in color density is apparent and the REVC shift is reliably evident. By choosing linker concentration of 15 μg/mL, as shown in Figure IV-6, *Salmonella* Typhimurium could be detected down to 10^1 CFU/400 μL.

IV-4. References

1. K. K. Alharbi and Y. A. Al-sheikh, *Saudi journal of biological sciences*, 2014, **21**, 109-117.
2. Y.-F. Chen, L. Jiang, M. Mancuso, A. Jain, V. Oncescu and D. Erickson, *Nanoscale*, 2012, **4**, 4839-4857.
3. S. Nayak, N. R. Blumenfeld, T. Laksanasopin and S. K. Sia, *Analytical chemistry*, 2016, **89**, 102-123.
4. P. Yager, G. J. Domingo and J. Gerdes, *Annual review of biomedical engineering*, 2008, **10**.
5. M. U. Ahmed, M. M. Hossain, M. Safavieh, Y. L. Wong, I. A. Rahman, M. Zourob and E. Tamiya, *Critical reviews in biotechnology*, 2016, **36**, 495-505.
6. R. Dragone, G. Grasso, M. Muccini and S. Toffanin, *Frontiers in public health*, 2017, **5**, 80.
7. S. K. Vashist, P. B. Luppa, L. Y. Yeo, A. Ozcan and J. H. Luong, *Trends in biotechnology*, 2015, **33**, 692-705.
8. P. Mandal, A. Biswas, K. Choi and U. Pal, *American Journal Of Food Technology*, 2011, **6**, 87-102.
9. S.-H. Seo, Y.-R. Lee, J. H. Jeon, Y.-R. Hwang, P.-G. Park, D.-R. Ahn, K.-C. Han, G.-E. Rhie and K.-J. Hong, *Biosensors and Bioelectronics*, 2015, **64**, 69-73.
10. L. Xiang, H. Wu, Z. Cui and J. Tang, *Analytical Letters*, 2019, **52**, 1966-1975.
11. H. Chen, K. Liu, Z. Li and P. Wang, *Clinica Chimica Acta*, 2019.
12. C. D. Chin, T. Laksanasopin, Y. K. Cheung, D. Steinmiller, V. Linder, H. Parsa, J. Wang, H. Moore, R. Rouse and G. Umviligihozo, *Nature medicine*, 2011, **17**, 1015.
13. P. Yager, T. Edwards, E. Fu, K. Helton, K. Nelson, M. R. Tam and B. H. Weigl, *Nature*, 2006, **442**, 412.
14. G. M. Whitesides, *Nature*, 2006, **442**, 368.
15. M. L. de Castro, J. Ruiz-Jiménez and J. Pérez-Serradilla, *TrAC Trends in Analytical Chemistry*, 2008, **27**, 118-126.
16. J. Ruzicka, *Analyst*, 2000, **125**, 1053-1060.
17. J. Wang and E. H. Hansen, *TrAC Trends in Analytical Chemistry*, 2003, **22**, 225-231.
18. M. Miró and E. H. Hansen, *Analytica chimica acta*, 2012, **750**, 3-15.
19. E. Mattio, F. Robert-Peillard, L. Vassalo, C. Branger, A. Margaillan, C. Brach-Papa, J. Knoery, J.-L. Boudenne and B. Coulomb, *Talanta*, 2018, **183**, 201-208.
20. P. Athanasatos and T. Costopoulos, *Mechanism and Machine Theory*, 2012, **50**, 64-89.
21. M. Giousouf and G. Kovacs, *Smart Materials and Structures*, 2013, **22**, 104010.

22. M. L. S. Silva, M. B. Q. Garcia, J. L. Lima and E. Barrado, *Talanta*, 2007, **72**, 282-288.
23. W. J. Kitsch, *Journal*, 2011.
24. S. Shoji, in *Microsystem technology in chemistry and life science*, Springer, 1998, pp. 163-188.
25. J. Fang, Q. Wang and N. Hu, in *Micro/Nano Cell and Molecular Sensors*, Springer, 2016, pp. 97-123.
26. T. C. Hinkley, S. Singh, S. Garing, A.-L. M. Le, K. P. N. Ny, J. E. Peters, J. N. Talbert and R. Sam, *BIOENGINEERING BACTERIOPHAGE FOR THE SENSITIVE & RAPID DETECTION OF BACTERIA IN WATER*, 2018, 147.
27. H. E. Indyk, E. A. Evans, M. C. B. Caselunghe, B. S. Persson, P. M. Finglas, D. C. Woollard and E. L. Filonzi, *Journal of AOAC International*, 2000, **83**, 1141-1148.
28. L. Y. Yeo, H. C. Chang, P. P. Chan and J. R. Friend, *small*, 2011, **7**, 12-48.
29. G.-H. Chen, W.-Y. Chen, Y.-C. Yen, C.-W. Wang, H.-T. Chang and C.-F. Chen, *Analytical chemistry*, 2014, **86**, 6843-6849.
30. Z. Guo, J. Duan, F. Yang, M. Li, T. Hao, S. Wang and D. Wei, *Talanta*, 2012, **93**, 49-54.
31. Y. Luo, J. Xu, Y. Li, H. Gao, J. Guo, F. Shen and C. Sun, *Food Control*, 2015, **54**, 7-15.
32. S. E. Magubane, S. Ntlhoro, M. Sabela, S. Kanchi, M. Mlambo, S. C. Onwubu, P. S. Mdluli and A. M. Asiri, *Journal of the Taiwan Institute of Chemical Engineers*, 2019, **101**, 159-166.
33. I. E. Sendroiu, S. F. Mertens and D. J. Schiffrin, *Physical Chemistry Chemical Physics*, 2006, **8**, 1430-1436.
34. J. Hahn, E. Kim, Y. S. You and Y. J. Choi, *Analyst*, 2019.
35. J. Hahn, E. Kim, Y. S. You, S. Gunasekaran, S. Lim and Y. J. Choi, *Journal of food science*, 2017, **82**, 2321-2328.
36. S. Lim, O. K. Koo, Y. S. You, Y. E. Lee, M.-S. Kim, P.-S. Chang, D. H. Kang, J.-H. Yu, Y. J. Choi and S. Gunasekaran, *Scientific reports*, 2012, **2**, 456.
37. Y. You, S. Lim, J. Hahn, Y. J. Choi and S. Gunasekaran, *Biosensors and Bioelectronics*, 2018, **100**, 389-395.
38. G. Frens, *Nature physical science*, 1973, **241**, 20.
39. K. C. Grabar, R. G. Freeman, M. B. Hommer and M. J. Natan, Analytical chemistry, 1995, **67**, 735-743.

국문 초록

현대사회에서 인간의 평균수명은 지속적으로 증가하고 있으며, 이에 따른 행복과 건강에 대한 관심이 크게 증가하고 있다. 전세계적인 이러한 현상은 자연스럽게 진단기술의 개발을 촉진시켰다. 특히, 바이오센서는 현장 진단용 기술로 큰 기대를 받고 있다. 분석물을 생체 인식 시스템을 이용하여 분석하는 장치인 바이오센서는 일반적으로 감지기, 변환기, 신호 분석 시스템 세 가지 요소로 구성된다. 바이오센서의 목표는 생물학적인 감지를 높은 민감도와 선택도로 구현하는 것이다. 의료 및 현장검사(point-of-care testing, POCT) 용을 시작으로 발전한 바이오센서의 진단기술은 식품안전, 군사, 환경 모니터링 등의 다양한 분야로 확대 · 응용되었다. 식품안전 분야에서의 바이오센서의 개발은 큰 어려움이 존재하는데, 그 이유로는 식품이 가지는 매우 다양하고 복잡한 matrix 때문이다. 즉, 식품은 종류도 다양하며, 그 안의 구성 matrix 도 매우 복잡 · 다양해서 바이오센서의 작동을 어렵게 한다. 따라서, 식품 안전분야의 바이오센서의 개발은 식품에 대한 이해를 토대로 연구개발되어야 한다. 즉, 식품안전분야에서는 전처리 과정이 적으며, 식품의 matrix 에 영향을 많이 받지 않으면서, 많은 양의 샘플을 처리할 수 있는 현장적용이 가능한

바이오센서의 개발이 필요하다. 또한, 현장 적용에 최적화되기 위해서는 장치의 소형화, 자동화, 간편화 등이 동반되어야 한다.

금 나노입자의 응집을 이용한 비색반응은 육안으로 신호분석을 할 수 있어서 특별한 분석장비가 필요하지 않다는 이유로 현장적용에 적합한 기술로 평가받고있다. 하지만 이 반응은 약 10^{10} ea/mL 이상의 농도의 금 나노입자를 이용해야만 하는 점과 분석물의 감지와 신호분석이 동시에 일어나는 특성이 맞물려서 민감도가 좋지 않다는 한계점이 존재한다. 이에 따라서, 이중기능링커(bi-functional linker), 동일한 의미인 스위치어블 링커(switchable linker)를 사용한 새로운 금 나노입자의 응집 시스템은 금 나노입자의 응집과 분석물과의 반응을 서로 독립시켜서 이러한 문제점을 해결함으로써, 현장 적용에 적합한 바이오센서로서 대두되었다.

본 연구에서는 이중기능링커를 활용한 금 나노입자의 응집반응으로 토마토에서 살모넬라 균(*Salomonella* Typhimurium)을 간단한 조작으로 45 분 이내에 10 cells/mL 이하로 검출할 수 있음을 보임으로서 식품산업현장에 적용가능성을 입증하였다. 또한, 1/10 희석한 serum 에서 단백질 바이오마커인 prostate-specific antigen 을 100 fg/mL 의 수준까지 검출 가능함을 보임으로서 다양한 분석물에 적용할 수 있음을 보였다. 마지막으로, 3-way valve chamber 와 주사기 필터를 적용한 소형화된 검출

장치를 통하여 살모넬라 균(*Salomonella* Typhimurium)을 검출함으로서, 이중기능링커의 금 나노입자 응집반응 시스템이 현장에 적용할 수 있음을 보였다. 물론 본 전략이 식품현장에서 사용하기 위해서는 자동화, 대량화, 안정성 등의 문제를 해결해야 할 것이다. 하지만, 간편하고, 민감하며, 매우 빠르게 분석물을 진단할 수 있다는 점에서 현장적용의 잠재력이 높다고 판단된다.

핵심어: 금 나노입자(Au NP), 응짐, 이중기능링커(BL), 현장검출, 육안

학 번: 2012-23392